Review

MicroRNA expression in animal models of amyotrophic lateral sclerosis and potential therapeutic approaches

Bridget Martinez[1, 2], Philip V. Peplow[3, *]

Abstract

A review of recent animal models of amyotrophic lateral sclerosis showed a large number of miRNAs had altered levels of expression in the brain and spinal cord, motor neurons of spinal cord and brainstem, and hypoglossal, facial, and red motor nuclei and were mostly upregulated. Among the miRNAs found to be upregulated in two of the studies were miR-21, miR-155, miR-125b, miR-146a, miR-124, miR-9, and miR-19b, while those downregulated in two of the studies included miR-146a, miR-29, miR-9, and miR-125b. A change of direction in miRNA expression occurred in some tissues when compared (e.g., miR-29b-3p in cerebellum and spinal cord of wobbler mice at 40 days), or at different disease stages (e.g., miR-200a in spinal cord of SOD1(G93A) mice at 95 days *vs.* 108 and 112 days). In the animal models, suppression of miR-129-5p resulted in increased lifespan, improved muscle strength, reduced neuromuscular junction degeneration, and tended to improve motor neuron survival in the SOD1(G93A) mouse model. Suppression of miR-155 was also associated with increased lifespan, while lowering of miR-29a tended to improve lifespan in males and increase muscle strength in SOD1(G93A) mice. Overexpression of members of miR-17~92 cluster improved motor neuron survival in SOD1(G93A) mice. Treatment with an artificial miRNA designed to target hSOD1 increased lifespan and improved muscle strength in SOD1(G93A) animals. Further studies with animal models of amyotrophic lateral sclerosis are warranted to validate these findings and identify specific miRNAs whose suppression or directed against hSOD1 results in increased lifespan, improved muscle strength, reduced neuromuscular junction degeneration, and improved motor neuron survival in SOD1(G93A) animals.

Key Words: amyotrophic lateral sclerosis; animal model; brain; brainstem; microRNA; motor neuron degeneration; spinal cord; therapeutic approaches

Introduction

The most common motor neuron (MN) disease in adults is amyotrophic lateral sclerosis (ALS) (Shaw and Eggett, 2000), with a worldwide annual incidence rate of approximately 2–3 cases per 100,000 people (Kiernan et al., 2011; Al-Chalabi et al., 2016). Irreversible and progressive degeneration of MNs in the motor cortex, brainstem and spinal cord characterize the clinical phenotype (Bucchia et al., 2015). Aggregations of misfolded proteins, disorders of axonal transport, mitochondrial dysfunction, excitotoxicity, neuroinflammation, and altered RNA processing are pathological characteristics of ALS (Brown and Al-Chalabi, 2017).

In most spinal-onset ALS patients, the MN subtype innervating distal limbs is the first to degenerate with patients initially experiencing muscle weakness or atrophy in the arms or legs (Kanning et al., 2010; Swinnen and Robberecht, 2014). Subsequently additional MN subtypes are affected and usually within 3–5 years after diagnosis patients experience complete paralysis and die from respiratory failure. Currently no effective treatments are available for ALS; thus, highlighting the need to further identify mechanisms that can serve as therapeutic targets. Riluzole is a previously approved drug for ALS and has a small beneficial effect on bulbar and limb function, improving patient survival by about two months (Miller et al., 2012). A new drug Edaravone approved by the US Food and Drug Administration showed efficacy in a small subset of individuals with ALS who met well-defined criteria. However, there was no indication that it might be effective in a wider population of ALS patients who do not meet the criteria (Abe et al., 2017).

Most ALS patients are classified as sporadic and only 5–10% of cases have a familial history (Renton et al., 2014; Chia et al., 2018). Mutations in or deletion of the Cu/Zn superoxide dismutase 1 (*SOD1*) gene are the most studied genetic causes of ALS (Rosen et al., 1993). Other genes associated with ALS include *TARDBP*, encoding transactive response DNA-binding protein 43 (*TDP-43*), fused in sarcoma (*FUS*), and *C9orf72* (Kabashi et al., 2008; Sreedharan et al., 2008; Yokoseki et al., 2008; Kwiatkowski et al., 2009; Vance et al., 2009; DeJesus-Hernandez et al., 2011). While 40% of familial ALS (fALS) patients carry a mutation in the *C9orf72* gene (Majounie et al., 2012), the large number and variety of identified *SOD1* mutations found in 20% of fALS cases have made this an extensively used experimental model (Renton et al., 2011, 2014).

Many of the identified ALS-associated genes encode for RNA-binding proteins such as TDP-43, FUS, and heterogeneous nuclear ribonucleoprotein A1 (Buratti et al., 2010; Kawahara

[1]Physical Chemistry and Applied Spectroscopy, Chemistry Division, Los Alamos National Laboratory, Los Alamos, NM, USA; [2]Department of Medicine, St. Georges University School of Medicine, Grenada; [3]Department of Anatomy, University of Otago, Dunedin, New Zealand
*Correspondence to: Philip V. Peplow, PhD, phil.peplow@otago.ac.nz.
https://orcid.org/0000-0001-5468-1989 (Philip V. Peplow)

and Mieda-Sato, 2012; Morlando et al., 2012). Moreover, many of these fALS-associated genes are involved in microRNA (miRNA) biogenesis (Guil and Caceres, 2007; Goodall et al., 2013; Gascon and Gao, 2014). MiRNA expression has been examined in MN diseases (Vance et al., 2009; Haramati et al., 2010; Butovsky et al., 2015; Emde et al., 2015; Parisi et al., 2016). An overall decrease of mature miRNAs and altered miRNA processing were found in postmortem spinal cord samples of ALS patients (Figueroa-Romero et al., 2016). Altered expression of specific miRNAs was observed in the cerebrospinal fluid (CSF), serum and leukocytes of ALS patients (De Felice et al., 2014; Freischmidt et al., 2015; Takahashi et al., 2015; Benigni et al., 2016; Tasca et al., 2016). While an altered miRNA expression in ALS patients and mouse models has been reported (Kye and Goncalves Ido, 2014; Eitan and Hornstein, 2016), the roles and sets of miRNAs involved in ALS are not fully known. Onset of MN loss in a fALS-SOD1(G93A) mouse model was shown to be accelerated by loss of the muscle-specific miRNA, miR-206 (Williams et al., 2009), but whether MN-specific miRNAs could serve as potential therapeutic targets is unclear. A large number of miRNAs have been shown to be dysregulated in various ALS tissues (Russell et al., 2013; Paez-Colasante et al., 2015; Figueroa-Romero et al., 2016) with an overall downregulation of miRNAs in MNs of ALS patients (Emde et al., 2015). MiRNAs have been found either upregulated or downregulated in ALS spinal cord, muscle tissue, and peripheral blood mononuclear cells (Kye and Goncalves Ido, 2014). Alterations in neuronal fate of cultured ependymal stem/progenitor cells isolated from the spinal cord of ALS mice were significantly associated with the expression of neural (miR-9, miR-124a) and cell cycle-related (miR-19a, miR-19b) miRNAs, and became more pronounced as the disease progressed (Marcuzzo et al., 2014). However, it is unclear to what extent these dysregulated miRNAs influence the disease onset, progression, and severity. Impaired RNA processing and stability may contribute to the development of ALS (Droppelmann et al., 2014). The aim of this review was to provide an analysis of recent literature on the expression levels and possible roles of miRNAs in ALS animal models and their potential for guiding therapeutic design.

Animal Models of Amyotrophic Lateral Sclerosis

Mouse and other animal models are necessary for studying ALS, which is a collection of diseases that involve different systems, including the immune system. Specific disease courses occur in different animal models, which is also likely in ALS patients. Thus, it is important to use different models to study ALS pathogenic mechanisms more completely. Two main types of animal models have been developed, toxin-induced models and genetic models.

Toxin-induced models
β-Sitosterol-β-D-glucoside treatment in mice
Dietary treatment of β-sitosterol-β-D-glucoside (BSSG), a common plant sterol present in high amounts in cycad flour, has been used to develop a mouse model of sporadic ALS (sALS). Progressive motor neuron degeneration occurred in mice fed the flour made from raw washed cycad seeds or the synthesized form of BSSG, and intensified after BSSG exposure was discontinued, The model mimicked many features of human ALS disease with loss of motor neurons, reduced neuromuscular junction (NMJ) integrity, astrocytosis, evidence of microgliosis, and neuronal cell death in pathologically relevant CNS regions (Wilson et al., 2002; Tabata et al., 2008). BSSG treatment in rats results in animals showing cognitive deficits marked by progressive degeneration in the substantia nigra pars compacta, and more closely resembles a parkinsonian phenotype (Van Kampen et al., 2015).

Genetic models
The wobbler mouse model
The wobbler mouse was the first proposed mouse model of ALS (Duchen and Strich, 1968) and it arose by spontaneous mutation in a C57BL/Fa mouse strain (Falconer, 1956). A single leucine to glutamine base pair exchange in the last exon of the vacuolar-vesicular protein sorting factor 54 gene was identified (Schmitt-John et al., 2005). Wobbler mice exhibit an ALS-like phenotype with muscle atrophy, unsteady gait, decreased body weight, and tremor. A major advantage of wobbler mice is they show nearly all clinical hallmarks of human ALS patients (Duchen and Strich, 1968; Bruijn et al., 2001). The only symptom lacking in the wobbler mice is frontotemporal dementia, which appears in ~10% of human ALS cases, and cannot be evaluated in the mouse model (Achi and Rudnicki, 2012). Pathologies in common with human ALS include axonal transport impairment, ubiquitin-positive protein aggregation, upper and lower MNs degeneration, and enlarged endosomes vacuolization (Duchen and Strich, 1968; Mitsumoto et al., 1990; Ferraiuolo et al., 2001; Dennis and Citron, 2009; Palmisano et al., 2011; Moser et al., 2013). In the first three postnatal weeks (from 0 to 20 days), no clinical abnormalities are seen in homozygous wobbler mice and no differences are observed between wobbler mice and wild type (WT) littermates (Ott et al., 2015). Following the preclinical stage (20 days of age), the first symptoms start to appear such as head tremor, unsteady gait or muscle weakness of the front limbs (Duchen and Strich, 1968; Boillee et al., 2003). At 40 days of age, the clinical phenotype is fully developed in homozygous wobbler mice (Saberi et al., 2016).

SOD1 animal models
Mice and rats with mutations in the SOD1 gene develop MN degeneration and muscle atrophy (Gurney, 1994). Although the exact pathological role of SOD1 in ALS is unclear, a series of transgenic mice carrying fALS SOD1 mutants has been established. NMJ dysfunction within limb muscles, with limb movement impairment, is seen very early as the first sign of disease onset in these mice (Pun et al., 2006). Subsequently, NMJs degenerate in the diaphragm (Rocha et al, 2013).

The SOD1(G93A) transgenic mouse model overexpresses the G93A mutated human SOD1 gene, and exhibits symptoms and neuropathological features similar to those of human ALS patients (Gurney, 1997). Skeletal muscle atrophy occurs in SOD1(G93A) mice at a very early stage in the absence of motor symptoms or neurodegenerative changes in brainstem MNs (Marcuzzo et al., 2011). A rapid degeneration of MNs leading to paralysis and death within the first 5 months of age occurs in this model (Nardo et al., 2016). Upper MN deficits are absent in this model.

While the SOD1(G93A) mouse model has been the most used and studied animal model of ALS, other SOD1 mouse models have been developed with mutations outside G93A (e.g., G37R, G85R, G86R) (Philips and Rothstein, 2015). These models develop adult-onset progressive MN disease, with varying degree of age of onset and disease progression rates. In SOD1(G93A) mice, disease onset usually occurs at 3 months of age and survival is to 4–5 months of age. By contrast, in SOD1(G37R) mice, disease onset usually occurs at 3.5–6 months of age and survival is to 7 months of age. For SOD1(G85R) mice, disease onset is at 8 months of age and survival is to 8.5 months of age.

FUS mouse models
Several FUS mouse models have been generated by insertion of human wild type FUS or knockout of FUS. Transgenic mice overexpressing wild type human FUS exhibited an early onset tremor followed by progressive hind limb paralysis and death by 12 weeks in homozygous animals. There was loss of large MNs from the spinal cord accompanied by denervation and

Review

muscle atrophy. Surviving MNs in the spinal cord had greatly increased cytoplasmic expression of FUS, with FUS-positive and ubiquitin-negative inclusions associated with astroglial and microglial reactivity. Cytoplasmic FUS inclusions occurred in the brain of transgenic mice without apparent neuronal loss and little astroglial and microglial activation. Hemizygous FUS overexpressing mice did not show any evidence of a motor phenotype or pathology (Mitchell et al., 2013).

FVB-C9orf72 BAC mouse model

A hexanucleotide repeat expansion in chromosome 9 open reading frame 72 was identified as a gene mutation associated with fALS and with those affected carrying between 23 and 5000 repeat sequences (Al-Chalabi and Hardiman, 2013; Haeusler et al., 2014). While many different rodent models of *C9orf72* have been developed, the FVB-C9orf72 BAC transgenic mouse model harboring a large repeat expansion (C9-500) was reported by Liu et al. (2016) to develop many features similar to ALS including paralysis, MN loss, impaired NMJ integrity, RNA foci formation, dipeptide repeat protein aggregation, TDP-43 cytoplasmic aggregation, and decreased lifespan. However, a recent study of C9orf72 BAC C9-500 mice of up to 1 year revealed no reproducible abnormalities in motor function, neuronal loss, or survival (Mordes et al., 2020), and these findings were consistent with the first investigations of C9orf72 BAC transgenic mouse models which were unable to detect motor deficits or decreased survival (O'Rourke et al., 2015; Peters et al., 2015). Possible explanations for the differences in findings include the housing environment may contribute to phenotypic manifestations in C9-500 animals or could be due to differences in genetic background on which the model was created. Furthermore, the study by Liu et al. (2016) employed relatively small numbers of C9-500 mice and controls, together with the relatively high frequency at which FVB/N-related phenotypes occur, raises the possibility that misassignment of effect to the C9-500 transgene may have occurred (Mordes et al., 2020). C9-BACexp mice containing the full human *C9orf72* gene with disease-associated expansion (~100–1000 repeats) exhibited pathological features observed in *C9orf72* expansion patients including widespread RNA foci and repeat-associated non-ATG translated dipeptides (O'Rourke et al., 2015).

TDP-43-Q331K mouse model

Approximately 20 different mouse models of TDP-43 have been developed (Lutz, 2018). The TDP-43-Q331K mouse model is based on mild overexpression of human mutant TDP-43 (Arnold et al., 2013), with the degenerative phenotype not caused by human wild type TDP-43. The TDP-43-Q331K model shows many ALS-like features such as progressive motor dysfunction, muscle atrophy, decreased NMJ integrity, and MN degeneration at 10 months of age. The motor phenotype only involves lower MNs, the progressive degeneration stops at 20 months, and the ALS-like outcomes do not cause death. In addition, no TDP-43 cytosolic aggregation or nuclear export occurs in this model (Arnold et al., 2013; Philips and Rothstein, 2015; Lutz, 2018). Ubiquitinated TDP-43 cytoplasmic inclusions have been observed in other mutant TDP-43 mouse models (Xu et al., 2010; Stribl et al., 2014).

MicroRNAs in Animal Models of Amyotrophic Lateral Sclerosis

We performed a PubMed search of articles published from January 2012 to August 2020 on the expression levels of miRNAs in animal models of ALS. In addition, we examined these articles for whether overexpression or suppression of specific miRNAs could alleviate ALS and thereby serve as therapeutic targets. The steps involved in the review and its contents are shown (**Figure 1**). A total of 19 articles were found for this review. Of these, 17 had been performed with

SOD1 mice, one with wobbler mice, and one with cynomolgus monkeys; in addition, of the studies using SOD1 mice, one had included SOD1 rats and one had included marmoset monkeys. The relevant findings from the research articles in the PubMed search are summarized as follows.
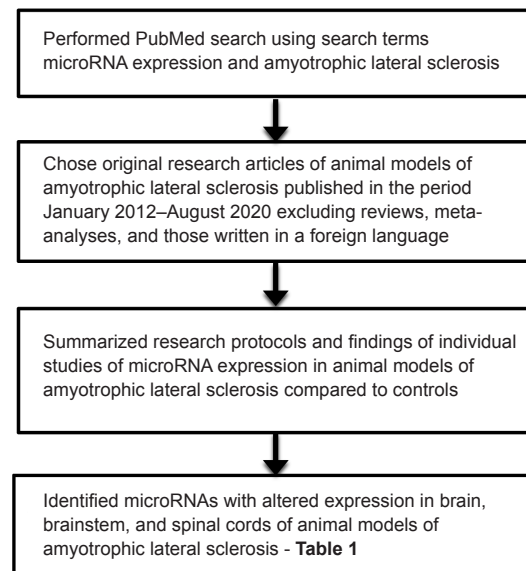

Figure 1 │ **Flow diagram to indicate how the review was performed and its contents.**

MiRNAs in spinal cord of SOD1(G93A) mice

Loffreda et al. (2020) found using RT-qPCR that the expression of miR-129-5p and miR-200c was increased at the early symptomatic stage (15 weeks of age) and that of miR-206 was increased at the pre-onset (10 weeks), early symptomatic (15 weeks), and end stage (22 weeks) of the disease in the lumbar spinal cord of SOD1(G93A) female mice.

The numbers of ChAT[on] MNs in SOD1(G93A) lumbar spinal cords were shown by Tung et al. (2019) to be relatively unaffected before 80 days of age and slightly decreased at 100 days of age. At 80 days of age, a significant downregulation of miR-17 expression in SOD1(G93A) MNs was found by RT-qPCR. At 100 days of age, the expression of ChAT was unchanged between the microdissected Ctrl and SOD1(G93A) MNs, but several members of the miR-17~92 cluster (miR-17, miR-18a, miR-20a) had significantly decreased expression in SOD1(G93A) MNs. Together with the downregulation of miR-17~92 cluster, an associated increase was observed in the expression of its targets *PTEN*, *Nedd4-2*, and *Ndfip1* in SOD1(G93A) MNs at 100 days of age.

Using *in situ* hybridization (ISH), Zhou et al. (2018) detected several gliosis-related miRNAs including miR-146a, miR-219, miR-21, and miR-124 in the spinal cord and brainstem of SOD1(G93A) mice. MiR-146a was significantly decreased but miR-129 was significantly increased at the three stages of disease (95, 108, and 122 days of age) in the ventral horn of the spinal cord and the hypoglossal, facial, and red motor nuclei of SOD1(G93A) mice compared with WT mice. MiR-21 was upregulated in the spinal cord but decreased in the red motor nuclei and facial and hypoglossal nerve nuclei at 95, 108, and 122 days of age in SOD1(G93A) mice compared with WT mice. The expression of several apoptosis-related miRNAs including miR-181a, miR-22, miR-26b and miR-34a in the spinal cord and brainstem of ALS transgenic mice was measured. There was an increased expression of miR-181a, whereas miR-22, miR-26b, and miR-34a had decreased expression at the three different stages of disease in the spinal cord and hypoglossal, facial, and red nuclei of SOD1(G93A) mice compared with WT mice. The expression of miR-

200a and miR-320 in the spinal cord and brainstem of ALS transgenic mice was also altered. MiR-200a was increased at 95 days but decreased at 108 and 122 days in the spinal cord and hypoglossal, facial and red nuclei of SOD1(G93A) mice compared with WT mice. MiR-320 was decreased at the three stages of disease in the spinal cord and hypoglossal, facial and red nuclei of SOD1(G93A) mice compared with WT mice. The level of these miRNAs in the oculomotor nerve nucleus was unchanged in SOD1(G93A) mice compared with WT mice. MiR-124-positive cells were found mainly in the ventral horn of the spinal cord and hypoglossal, facial, and red nuclei of SOD1(G93A) mice. The expression of miR-124 was increased at 95 days but decreased at 108 and 122 days in the spinal cord and hypoglossal, facial, and red nuclei of SOD1(G93A) mice compared to WT mice. The expression of selected miRNAs in the spinal cord was confirmed by qRT-PCR. MiR-219, miR-21 and miR-181a were increased at 95, 108, and 122 days of age in SOD1(G93A) mice compared with WT mice, while miR-146a, miR-22, miR-26b, miR-34a, and miR-320 were decreased at these three different stages of disease. In addition, levels of miR-200a and miR-124 were increased, while those of miR-200a and miR-124 were decreased, in SOD1(G93A) mice at 95 days of age.

Higher levels of hSOD1 expression were observed in SOD1(G93A) male mice at both presymptomatic (4–6 weeks of age) and symptomatic phase (12–14 weeks) of the disease than in WT animals by Cunha et al. (2018). The number of MNs was only decreased in SOD1(G93A) mice at the symptomatic stage. Pyknotic basophilic necrotic/apoptotic MNs were shown by H&E staining at the symptomatic stage of SOD1(G93A) mice, together with an increased number of glial cells. In the presymptomatic stage, an increased expression of miR-155 was observed by RT-PCR, together with a decreased expression of its direct target, the suppressor of cytokine signaling 1 (SOCS1) (Pathak et al., 2015). The existence of a neuroinflammatory status after disease onset was indicated by the sustained increase of miR-155, as well as decreased expression of anti-inflammatory associated marker SOCS1, together with Arg1 subexpression. Decreased GFAP expression indicated an astrocyte abnormality (Diaz-Amarilla et al., 2011). Various proinflammatory miRNAs such as miR-155, miR-21, miR-146a, miR-125b, and miR-124 have been associated with different phenotypes and functions of microglia in ALS (Brites and Vaz, 2014). Among them, only miR-155 was significantly upregulated in the spinal cord of asymptomatic SOD1(G93A) mice. This indicated that miR-155 upregulation occurred earlier, before disease onset, and in the absence of other common proinflammatory miRNAs. In the symptomatic stage, there was evidence of an increased inflammatory status in the spinal cord of SOD1(G93A) mice as shown by upregulated inflammatory signaling pathways involving NF-κB and its active phosphorylated form pNF-κB, increased *Nlrp3*, *IL-1beta*, *Tnfa* expression, as well as elevated HMGB1 cellular content. Increased expression of miR-155 was observed, but at this stage together with miR-125b, miR-146a, miR-21, and miR-124 significantly increased expression. MiR-155 and miR-125b are associated with proinflammatory responses and NF-κB activation (Ponomarev et al., 2013; Volonte et al., 2015; Cunha et al., 2016). MiR-146a and miR-21, also produced after NF-κB activation, act as feedback negative regulators to restrain microglia activation (Saba et al., 2012; Ponomarev et al., 2013). MiR-124 also influences microglia to adopt either a surveilling state or an anti-inflammatory phenotype (Ponomarev et al., 2011, 2013).

Hoye et al. (2017) found that six miRNAs were increased in either spinal cord or brainstem MNs compared with all other neurons in SOD1(G93A) mice. Using individual RT-qPCR assays at a higher power (*n* = 6), miR-218-5p, miR-218-2-3p, miR-138, miR-133a, miR-1193 had increased expression. MiR-218-5p and its lesser abundant 3p strand

had the greatest increase in adult MNs compared with all other spinal cord neurons. The increase of miR-218 in adult mouse spinal cord MNs was confirmed by ISH. MiR-218 was detected principally in the ChAT⁺ MNs in the anterior horns of the spinal cord but not in other cell types. RT-qPCR was performed on SOD1(G93A) spinal cord collected at 56, 84, 105, 126, and 147 days of age, as well as end stage (indicated by an animal's inability to right itself within 30 seconds). In the SOD1(G93A) mouse model, disease onset typically occurs at ~130 days of age as marked by time to peak weight. The MN-enriched miRNAs miR-218 and miR-138 had a significant temporal depletion in SOD1(G93A) mouse spinal cords beginning as early as 126 days of age, and was maximized in the end stage. Pan-neuronal enriched miRNAs miR-382 and miR-672 were decreased but not significantly depleted in ALS mouse model spinal cord, even at end stage. In ALS model rats, disease onset similarly occurred between 120 and 140 days of age, and as in ALS mice, MN-enriched miRNAs were more significantly depleted than pan-neuronal miRNAs in SOD1(G93A) rat spinal cords. In whole SOD1(G93A) mouse spinal cord tissue, miR-218 was not significantly depleted until 126 days of age. MiR-218 levels were not significantly changed in the surviving MNs from the presymptomatic (70 days) to symptomatic (140 days) time points in ALS mice. By miR-218 ISH using spinal cord tissue from 140 days of age SOD1(G93A) and littermate control mice, the miR-218 fluorescence signals were also not significantly different, but the numbers of ChAT⁺ MNs per unit area were significantly altered, confirming that ChAT⁺ MNs were lost in ALS mouse spinal cords.

Parisi et al. (2016) observed by RT-PCR that the expression of miR-125b, similarly to that of NADPH oxidase 2 (NOX2) mRNA, was significantly increased in lumbar spinal cord of SOD1(G93A) mice at end stage (~23 weeks of age) compared to non-transgenic mice, whereas the level of A20 protein was significantly decreased as indicated by Western blotting analysis. The enzyme A20 has anti-inflammatory functions and is a feedback-loop suppressor of NF-κB signaling to stop the inflammatory response of several stimuli such as TNF-α and LPS (Boone et al., 2004; Turer et al., 2008; Coornaert et al., 2009).

Using RT-PCR, Marcuzzo et al. (2015) showed at 18 weeks the expression levels of miR-9 and miR-124a, but not miR-134, were significantly decreased, whereas miR-19a and miR-19b expression levels were significantly increased, in SOD1(G93A) whole spinal cord compared to WT-SOD1 spinal cord. Expression of miR-125b and miR-219 tended to be increased (although not statistically significant) in cervical, thoracic and lumbar spinal cord of SOD1(G93A) mice compared to control mice.

Dobrowolny et al. (2015) examined the expression of miRNAs in the lumbar spinal cord of Myosin Light Chain (MLC)/ SOD1(G93A) mice overexpressing mutant SOD1 gene under the control of MLC muscle specific promoter, 4 months of age, and FVB (Friend leukemia virus B) (control strain), 4 months of age. By RT-PCR, the expression of miR-133a, miR-133b, miR-9, miR-29, miR-330, and miR-1 was significantly decreased in the spinal cord of MLC/SOD1(G93A) mice compared to WT mice. Also, by RT-PCR for mRNA expression of genes involved in the myelination process, Pmp22, Prx, Mpz, Egr2 were significantly increased in the spinal cord of MLC/SOD1(G93A) mice, while Opalin was significantly decreased, compared to WT mice, consistent with these factors being targets of specific miRNAs that control denervation and reinnervation processes.

Using RT-qPCR, Nolan et al. (2014) found miR-29a to be increased in lumbar spinal cord from SOD1(G93A) mice at presymptomatic (70 days of age) and symptomatic (90 days of age) phase compared to SOD1 WT mice. The RT-qPCR analysis was validated by ISH using miR-29a-specific digoxigenin-labeled hybridization probes. MiR-29a was shown

to be expressed in the gray matter of the lumbar spinal cord. Expression of miR-29a was present in SOD1(G93A) mice at 70 days of age, with very weak miR-29a staining in sections from WT mice. Overlap in miR-29a expression and the position of Nissl-stained MNs on consecutive sections suggested that miR-29a was expressed in MNs, among other cell types.

Zhou et al. (2013) found by RT-qPCR that miR-9 levels in the spinal cord of SOD1(G93A) mice were significantly higher than those in WT mice at early (95 days of age), middle (108 days) and late (122 days) stages of the disease. ISH indicated that miR-9 was localized in the cytoplasm of the positive cells. The miR-9-positive cells were mainly detected in the gray matter of the ventral horn and the dorsal horn of the spinal cord of SOD1(G93A) and WT mice at the different time points, with the majority being located in the gray matter of the ventral horn, the site of neurodegeneration. The number of miR-9-positive cells was significantly increased at 95, 108, and 122 days of age in the SOD1(G93A) mice compared to WT mice. MiR-9 is involved in the proliferation and differentiation of neural stem cells (NSCs).

By microarray analysis, Koval et al. (2013) showed that 12 miRNAs were significantly increased in the spinal cord of SOD1(G93A) mice at end stage, including miR-155.

MiRNAs in cortical tissue of SOD1(G93A) mice
A significantly decreased expression of both NeuN and ChAT proteins was reported by Gomes et al. (2019) in cortical tissue from SOD1(G93A) mice at symptomatic stage, 12–14 weeks of age, but not at presymptomatic stage, 4–6 weeks, indicating a pronounced loss of neurons, mainly of MNs (~40%). A significantly decreased expression of the presynaptic SYP and postsynaptic PSD-95 proteins occurred at symptomatic stage. As miR-124 was shown to regulate synaptic structure and function (Hou et al., 2015) and miR-125b to be involved with neurite outgrowth (Le et al., 2009), their expression was measured in cortical tissue by RT-PCR. The expression of miR-124 was not altered, but that of miR-125b was significantly decreased at symptomatic stage. MiRNAs have been shown to play a critical role in neuroinflammation and differentially expressed in ALS (Volonte et al., 2015). Expression of both miR-21 and miR-146a in the cortical tissue of SOD1(G93A) mice was significantly decreased at symptomatic stage. MiR-146a expression was also significantly decreased at presymptomatic stage, highlighting miR-146a as an early biomarker of the disease. Expression of miR-155 was significantly decreased at symptomatic stage compared to presymptomatic stage, indicating a decrease in miR-155 expression with disease progression in the cerebral cortex.

MiRNAs in whole brain, brain regions of SOD1(G93A) mice
Using RT-PCR, Marcuzzo et al. (2015) showed that the expression levels of miR-9, miR-124a, and miR-19b did not differ significantly between whole brains of SOD1(G93A) mice at 8 weeks of age (presymptomatic), B6.SJL and WT-SOD1 mice, while that of miR-19a was significantly downregulated in ALS brain. However, at 18 weeks (late stage disease), expression levels of miR-9, miR-124a, miR-19a and miR-19b were significantly higher in SOD1(G93A) brains than control brains. In addition, miR-9 was significantly upregulated in SOD1(G93A) brain compared to 8 weeks, while miR-19a was significantly downregulated in SOD1(G93A) brain compared to 8 weeks. MiRNA expression was examined in specific brain regions of 18-week-old ALS mice concerned with neurogenesis (SVZ and hippocampus) and those affected by ALS (primary motor cortex and brainstem MN). MiR-124a expression was significantly higher in SVZ, hippocampus, primary motor cortex, and brainstem MN of ALS than WT-SOD1 mice. MiR-9 expression was significantly lower in SVZ and hippocampus, and significantly higher in primary motor cortex and brainstem MN in ALS compared to WT-SOD1 mice. MiR-19a expression

was significantly decreased in hippocampus and brainstem MN and significantly increased in primary motor cortex of SOD1(G93A) mice compared to control. MiR-19b expression was significantly increased in hippocampus and significantly decreased in primary motor cortex and brainstem MN of SOD1(G93A) mice compared to control. MiR-125b expression was significantly decreased in SVZ and hippocampus and significantly increased in primary motor cortex of SOD1(G93A) mice compared to control. MiR-219 expression was significantly decreased in SVZ of SOD1(G93A) mice compared to control.

MiRNA biogenesis pathway in the brain and spinal cord of SOD1(G93A) mice
Russell et al. (2018) found no differences in the mRNA levels of *Drosha* and *Xpo5* in brain tissue or cervical, thoracic, and lumbar regions of the spinal cord in SOD1(G93A) male mice at 99–137 days of age compared to the same tissue in WT mice. The mRNA levels of ALS-related genes that regulate the miRNA biogenesis pathway were measured. Except for an increase in mRNA level of *Fus* in the lumbar region of the spinal cord in SOD1(G93A) mice at 99–137 days, there were no differences in the brain tissue or in the cervical, thoracic, and lumbar regions of the spinal cord of SOD1(G93A) mice compared to the same tissue in WT mice.

MiRNAs in the spinal cord of wobbler mice
In a study by Klatt et al. (2019), cervical spinal cord was collected from WT and wobbler mice at presymptomatic (0 days of age, i.e., at birth) and stable symptomatic phase (40 days of age). By qRT-PCR, a highly significant upregulation of miR-29b-3p was found in the spinal cord of wobbler mice at 0 days of age, and a highly significant downregulation at 40 days of age. By ISH, miR-29b-3p staining was mainly within the gray matter of the spinal cord of WT mice. By qPCR, no alteration in mRNA levels of BCL-2-modifying factor (BMF) in the spinal cord of wobbler mice occurred at 0 and 40 days of age. There was a significant decrease of BMF protein expression in the spinal cord of wobbler mice at 0 days of age followed by a nonsignificant decreased protein expression at 40 days of age.

MiRNAs in the cerebellum of wobbler mice
Klatt et al. (2019) collected cerebellar tissue from WT and wobbler mice at presymptomatic (0 days of age, i.e., at birth) and stable symptomatic phase (40 days of age). Using qRT-PCR analysis, a highly significant decrease of miR-29b-3p expression occurred in the cerebellum of wobbler mice at 0 days of age, together with a highly significant increase of miR-29b-3p expression at 40 days of age. ISH using specific locked nucleic acid (LNA) mRNA detection probes showed that in the cerebellum miR-29b-3p was chiefly expressed in large cells located in the Purkinje cell layer in both WT and wobbler mice. Expression in small cells located in the white matter was also detected in wobbler mice. Cells with a large cell body, which pointed to MNs, expressed miR-29b-3p. A strongly reduced, barely recognizable, staining of miR-29b-3p was shown in the gray matter of wobbler mice. MiR-29b-3p targets BMF and other members of the apoptotic pathway. By qPCR, mRNA levels of BMF were significantly altered in the cerebellum at both 0 and 40 days of age. An increased amount of BMF mRNA was found in wobbler mice at 0 days of age, whereas mRNA levels were significantly decreased at 40 days of age. A significant increase in the level of BMF protein occurred in the cerebellum at 0 days of age, and a significant decrease of BMF protein expression was shown at 40 days of age.

MiRNAs as potential therapeutic targets in SOD1(G93A) mice
Loffreda et al. (2020) treated adult SOD1 mice (with a nearly equal number of males and females) with an intracerebroventricular (i.c.v.) injection of a morpholino (MO)

sequence targeting the miR-129-5p precursor, miR-129-1 (40 nmoles, $n = 14$) or ctr-MO ($n = 12$) at the early symptomatic phase (80 days of age). The ability of MO in decreasing miR-129 expression was shown by treating WT pups i.c.v. with 24 nmoles MO and harvesting spinal cords after 1 week when RT-qPCR analysis showed a significant decrease of miR-129-5p expression levels after treatment. ELAVL4/HuD mRNA is a target of miR-129-5p, and there was a significant increase in the level of the RNA-binding protein ELAVL4/HuD in the same mice. The lifespan of MO-treated SOD1 mice was significantly increased and muscle strength was also increased. At 120 days of age there was a trend toward reduced MN loss in the lumbar spinal cord of MO-treated SOD1 mice and a significant increase in the number of fully innervated NMJs compared to ctr-SOD1 mice.

MiR-17~92 was overexpressed in the whole spinal cord of SOD1(G93A) mice by intrathecal injection of a self-complementary adeno-associated vector serotype 9 (scAAV9) at 60 days of age by Tung et al. (2019). The efficiency of virus injection was tested by injecting scAAV9-GFP to Ctrl mice, and sustained GFP expression was observed in spinal MNs and also in some dorsal cells at 40 days post-injection. Pronounced induction of exogenous miR-17~92 in the spinal cord of Ctrl and SOD1(G93A) mice injected with scAAV9-GFP was verified by ISH of miR-17 as well as RT-qPCR quantification of miR-17~92 members in the lumbar spinal cord. Measurement of evoked compound muscle action potential (CMAP) in gastrocnemius muscle was performed. At 60 days of age, SOD1(G93A) mice had just started to show MN denervation and exhibited a slightly compromised CMAP amplitude. AAV9-miR-17~92 treatment significantly increased the CMAP response at 120 and 140 days of age but had not yet improved to the level of Ctrl mice. The data suggested that miR-17~92 overexpression enhanced MN survival significantly rather than promoted MN reinnervation, and also increased survival of the mice.

Butovsky et al. (2015) produced F2-SOD1(G93A)/miR-155$^{-/-}$ and SOD1(G93A)/miR-155$^{+/-}$ mice which had a deletion of one or two miR-155 alleles. Genetic deletion of miR-155 increased lifespan by 51 days in females ($n = 9–10$/group) and by 27 days in males ($n = 9–10$/group), extended the time to reach a neurologic score of 1 by 62 days in females and 58 days in males, improved rotarod performance, decreased body weight loss, and delayed early and late disease onset in females. Early phase onset was delayed in males, but late phase was not significantly affected by genetic deletion of miR-155. SOD1 mice were treated with anti-miR-155 given both peripherally and intraventricularly to assess whether treatment affected miR-155 targeted genes and increased lifespan. LNA-anti-miR-155 and scrambled LNA-anti-miR-155 were used. 2 mg/kg of anti-miR-155 was administered intraperitoneally beginning at disease onset as defined by body weight loss of 5% of mouse maximal weight (82 days of age) twice weekly (82, 85, 92, 95, 103 days of age) for a total of 5 injections (ending on day 103). Increased rotarod performance, delayed time to reach a neuroscore of 1 (6.5 days), and increased survival (11 days) were observed in peripherally treated animals. In addition, 2 mg/kg of anti-miR-155 was administered at disease onset as defined by body weight loss (90 days of age) with one injection given into the lateral ventricle. Increased rotarod performance, delayed time to reach a neuroscore of 1 (7 days), and increased survival (3 days) were observed. CNS treatment with anti-miR-155 derepressed miR-155 targeted genes in spinal cord microglia.

Nolan et al. (2014) examined miR-29a knockdown after stereotactic injection of 0.12, 0.5 or 1.0 nmole miR-29a-specific antagomir or control scrambled sequence. By RT-qPCR, the 1.0 nmole dose gave consistent knockdown across cortex, hippocampus and lumbar spinal cord tissue when compared to scrambled antagomir. MiR-29a knockdown was significant in the cortex and hippocampus compared to scrambled-treated mice at 10 days post-injection. Knockdown was also found in the lumbar spinal cord of these animals. MiR-29a knockdown remained significant in the cortex with some knockdown still present in the hippocampus and lumbar spinal cord at 30 days post-injection. The 1.0 nmole miR-29a antagomir was administered at 70 days of age to the CNS of SOD1(G93A) and SOD1 WT mice via i.c.v. injection and the disease progression monitored over time. A significant delay in motor dysfunction with knockdown of miR-29a could not be identified. The paw grip endurance test was used to assess the onset and progression of motor symptoms in SOD1(G93A) mice. A loss of grip strength over time occurred in both male and female transgenic mice treated with scrambled antagomir. Grip strength tended to be maintained longer in miR-29a antagomir-treated transgenic males and females than scrambled antagomir-treated mice; all transgenic animals declined in grip strength over time. SOD1(G93A) mice treated with miR-29a antagomir tended towards an increased lifespan compared to treatment with scrambled antagomir. While male mice treated with miR-29a antagomir showed a trend towards increased lifespan, female mice had no change in lifespan following treatment with miR-29a antagomir.

In a study by Koval et al. (2013) a large cohort of SOD1(G93A) mice at 60 days of age were treated with continuous intraventricular infusion of anti-miR-155 ($n = 22$), scrambled control anti-miR ($n = 21$), or saline ($n = 20$). Any peripheral role of miR-155 was accounted for by supplementing the CNS treatment with weekly anti-miR or saline intraperitoneally injections. Onset of disease was taken as the age when weight peaked and/or when a neurological score of 1 was observed indicated by abnormal hind limb motility. Treatment and monitoring continued until the animal reached the end stage, which was when the mouse was no longer able to right itself after being placed on its side within 30 seconds. No significant change in disease onset was observed, but survival was significantly increased in the anti-miR-155-treated mice which had a 9.5 day increase over saline-treated mice. The anti-miR-155-treated animals had a disease duration 14.5 days longer than saline-treated mice and 11 days longer than scrambled control anti-miR animals. There was no significant difference in survival or disease duration between scrambled-treated and saline-treated animals.

hSOD1 silencing in SOD1(G93A) mice and rats

Keeler et al. (2019) randomly assigned SOD1(G93A) mice to be treated with AAVrh10-H1-miR(SOD1) ($n = 8$, 7F/1M) or PBS ($n = 7$, 6F/1M), and littermate non-transgenic animals ($n = 8$, 7F/1M) received PBS. The AAVrh10-H1-miR(SOD1) vectors (AAV-miR(SOD1)) targeted the human SOD1 sequence. Vector doses were 1×10^{11} vector genomes (vg) per animal and were injected into the tongue and intrapleural space for a total vector dosage of 2×10^{11} vg per animal. SOD1(G93A) animals were injected at approximately 60 days of age with either AAV-miR(SOD1) or PBS. Treatment with AAV-miR(SOD1) caused a significant silencing of *SOD1* mRNA by 64% in the tongue and 80% in the diaphragm. The lung had a 35% reduction of *SOD1* mRNA. There was pronounced silencing systemically in the liver, heart, and hind limb with a significant decrease in expression of 86%, 87%, and 89%, respectively. The medulla and spinal cord also showed suppression of *SOD1* mRNA ranging from 23% to 45% but not statistically significant. Targeting the respiratory system by AAV-miR(SOD1) significantly increased survival by an average of 50 days compared to untreated SOD1(G93A) mice. Weight gain was significantly improved in treated compared to untreated SOD1(G93A) mice, with some treated mice maintaining weight until 190 days of age. AAV-miR(SOD1)-treated SOD1(G93A) mice had a slower neurological decline compared to untreated SOD1(G93A) mice. Less rapid deterioration of muscle strength

occurred in AAV-miR(SOD1)-treated SOD1(G93A) mice compared to untreated SOD1(G93A) mice. Breathing decline was lessened in the AAV-miR(SOD1)-treated SOD1(G93A) mice compared to untreated SOD1(G93A) mice.

SOD1(G93A) rats at 65 days of age were injected with an antisense oligonucleotide (ASO) against hSOD1, scrambled ASO, or artificial CSF (aCSF) between L4 and L5 of the lumbar spinal cord by Hoye et al. (2017). At 50 days after treatment with SOD1 ASO, hSOD1 mRNA was significantly decreased (~75%) in the lumbar spinal cord of these animals and hind limb grip strength was preserved. MiR-218 CSF levels were not reduced in scrambled ASO-treated rats but were markedly lowered in the hSOD1 ASO-treated group compared with aCSF-treated littermate controls. Previously published data suggested that miR-218 levels were increased in CSF during MN disease in SOD1(G93A) rats (Howland et al., 2002). The miR-218 CSF levels were selectively responsive to MN function-sparing therapy as shown by CSF levels of neuronal miR-132 and miR-124 being unchanged by SOD1 ASO treatment. Treatment of non-transgenic rats with aCSF, scrambled, or hSOD1 ASO did not affect miR-218 CSF levels. Increased miR-218 CSF levels due to MN loss were consistent with ALS MNs dying by necrosis and subsequently releasing miR-218 and other cellular components. This was tested using primary mouse MNs treated with sodium arsenite whereby miR-218 was increased temporally in the media and this correlated with lactate dehydrogenase activity, an indicator of cell death.

In a study by Stoica et al. (2016), an AAV9 artificial miRNA against hSOD1 was delivered i.c.v. to SOD1(G93A) mice on postnatal day 0–1. Human SOD1 mRNA levels in spinal cord were decreased up to 50% with no significant difference between cervical, thoracic, and lumbar regions. hSOD1 mRNA levels were reduced by > 80% in the heart and gastrocnemius muscle, but were unchanged in the liver and lung. There were no changes in the levels of mouse SOD1 mRNA in thoracic spinal cord. Using multiplex ISH, the intensity of hSOD1 mRNA signal was considerably reduced in cells expressing GFP mRNA both in motor cortex and spinal cord. Median survival in AAV9-amiR-SOD1 mice was significantly increased by 50% from 137 days for untreated SOD1(G93A) mice to 206 days. Untreated SOD1(G93A) mice developed hind limb paralysis but AAV9-treated SOD1(G93A) mice did not show signs of paralysis or movement impairment. Quantitative electrophysiological measures were used to assess neuromuscular function. The needle electromyography (EMG) scores of non-transgenic control animals were zero while untreated SOD1(G93A) animals scored in the 3 to 5 range, which corresponded to extensive acute muscle denervation. In contrast, AAV9-treated SOD1(G93A) mice scored 0 to 2 throughout the experiment. Examination of the sciatic nerves of end stage untreated SOD1(G93A) mice, AAV9-treated SOD1(G93A) and non-transgenic mice at 135 days of age revealed an extensive axonal loss in untreated SOD1(G93A) mice, whereas the sciatic nerves of AAV9-treated SOD1(G93A) and non-transgenic mice were indistinguishable. At end stage the distribution of ventral root axon size in AAV9-treated SOD1(G93A) mice was between that in untreated SOD1(G93A) and non-transgenic mice. The numbers of large and small diameter fibres in the ventral roots of AAV9-treated SOD1(G93A) mice was significantly different from untreated SOD1(G93A) mice and non-transgenic controls. The AAV9-treated SOD1(G93A) mice displayed considerable preservation of axonal integrity. The number of MNs in the ventral horn of lumbar spinal cord at end stage was quantified by counting ChAT^{+} neurons. A significant reduction in the number of ChAT^{+} neurons occurred in the end stage spinal cords of untreated SOD1(G93A) mice compared to control non-transgenic nice. By contrast, there was no significant difference between end stage AAV9-treated SOD1(G93A) and non-transgenic mice. MN death in both

human and mouse ALS is accompanied by neuroinflammation characterized by activation of astrocytes and microglia. The onset of microgliosis and astrocytosis was markedly delayed by AAV9-mediated silencing of hSOD1 in the SOD1(G93A) mice. There was a small increase in activated Iba1^{+} microglia and GFAP[+] reactive astrocytes in the spinal cord of AAV9-treated SOD1(G93A) mice at 135 days of age compared to non-transgenic control animals at 260 days.

Borel et al. (2016) designed an artificial miRNA miR-SOD1 based on the backbone of cellular miR-155 that targeted human SOD1. It was tested *in vivo* after rAAV-mediated delivery in SOD1(G93A) mice and compared the efficacy of pol II (chicken beta actin or CB) and pol III (U6) promoters. With either promoter, rAAVrh10-mediated delivery of miR-SOD1 via the tail vein to adult pre-onset SOD1(G93A) mice (56–68 days of age) extended survival. A significant extension in survival (22 days, or 20%) was observed in the group treated with the CB-driven construct (130 days) compared with an age-matched, gender-matched control group (108 days). Survival was extended to a greater extent by the CB-miR-SOD1 treatment in the subset of females (34 days, or 32%). A more robust extension of survival (27 days, or 21%) was observed in the group treated with the U6-driven construct (158 days) compared with age-matched, gender-matched littermates (131 days). There were no signs of toxicity in either group. For the CB-driven construct, the delay in disease onset of 11 days (12.5%) was not statistically significant (88 days for the control group *vs*. 99 days with treatment). By contrast, the U6-driven construct achieved a significant 31-day (31%) delay in onset (from 100 to 131 days) for the treated group. Disease duration was increased by treatment with the CB-miR-SOD1 construct from 18 to 35 days (94%). A similar disease duration was observed for the U6-miR-SOD1-treated (34 days) and the untreated (33 days) group, which indicated the increased survival in this group could be attributed primarily to a delay in disease onset. The treatment efficiently delayed muscle wasting and significantly maintained two and four limbs' strength. Motor skills were significantly preserved by the treatment as indicated by rotarod performance in mice (120 days or more of age).

Silencing of SOD1 by artificial miRNA in cynomolgus and marmoset monkeys
In a study by Borel et al. (2018), miR-SOD1 was administered intrathecally using AAV.rh10 vector to male cynomolgus monkeys closely matched in age and body weight. The quantity of miR-SOD1 in the spinal cord increased with the relative strength of the promoter (CB < H1 < U6). To precisely assess silencing in the MNs, an average of 400 cells were microdissected using laser capture. A significant silencing was shown in MNs with a 1.7-fold and 1.6-fold decrease of SOD1 expression in the H1 and U6 groups, compared with the CB group, respectively, in the cervical spinal cord, a 2.1-fold and 2.5-fold decrease in the thoracic spinal cord, and a 3.6-fold decrease in the H1 versus CB in the lumbar spinal cord. Lumbar spinal cord sections were stained with anti-GFP and anti-SOD1 antibodies. A non-injected control primate showed no GFP expression but strong SOD1 expression in MNs. Animals injected with the preclinical H1 vector (that included GFP) showed GFP expression in most but not all MNs, confirming that rAAVrh.10 targets MNs. The MNs expressing the GFP protein were not expressing SOD1, whereas GFP-negative MNs in the same tissue sections had SOD1 protein. To assess silencing of SOD1 in MNs, cells were laser captured and used to isolate RNA and subsequently quantify SOD1 expression. At 92 days after injection, silencing exceeded 30% in the CB group and 60% in the H1 group in the lumbar section of the spinal cord. The thoracic section showed an intermediate degree of silencing, while the cervical section had about 35% silencing in the CB group and about 45% in the H1 group.

In a previous study by Borel et al. (2016), nine marmosets of similar age (less than 4 years old) and body weight, and with low levels of neutralizing antibody against AAVrh10, received an intrathecal injection at lumbar level of rAAVrh10 encoding one of three constructs CB-GFP, CB-miR-SOD1, and U6-miR-SOD1. The animals were divided into three equal-sized, gender-matched groups, and euthanized at 18-23 days post injection. The females were subsequently excluded from analysis based on uncertainty of needle placement (shown by absence of tail-flick response). MNs were isolated from sections of the spinal cord by laser-capture microdissection. By RT-PCR to quantify SOD1 mRNA levels, SOD1 levels in MNs were decreased with the CB-miR-SOD1 by 21% in the lumbar region and 8% in the cervical region. In addition, SOD1 levels were decreased with the U6-miR-SOD1 by 93% in the lumbar, 65% in the thoracic, and 92% in the cervical region of the spinal cord. There was a positive correlation of the levels of SOD1 silencing with the levels of mature miR-SOD1 expression in the lumbar spinal cord. In the pons and medulla, SOD1 levels were lowered by 20% with the CB-miR-SOD1 and by 55% with the U6-miR-SOD1.

The findings from the studies in SOD1(G93A) and wobbler mice are summarized in **Tables 1** and **2**.

Discussion

A number of studies have been performed on ALS pathogenic mechanisms using different models but a common pathophysiological mechanism that would aid therapeutic advances has not yet been identified. A familial, genetic background is only detectable in about 10% of patients (fALS), and most of the cases occur sporadically without familial connection (sALS) (Ajroud-Driss et al., 2015). A molecular pathway leading to selective MN degeneration in fALS and sALS is still to be elicited (Cabellero-Hernandez et al., 2016; Taylor et al., 2016). Previous studies have indicated that a programmed mechanism of cell death similar to apoptosis is responsible for MN degeneration in ALS (Martin, 2000; Moser et al., 2013; Dahlke et al., 2015; Rohm et al., 2019). Several inflammatory pathways have been implicated in the progression of the disease and MN degeneration (McCombe et al., 2011). Cytoplasmic inclusions or aggregates in degenerating MNs impair the normal protein homeostasis and promote cellular stress (Saxena and Caroni, 2011). This abnormal protein aggregation has been observed in both fALS and sALS patients (Gruzman et al., 2007) and linked with decreased patient survival (Wang et al., 2008). About 20% of fALS and 1–3% of sALS patients carry a mutation in the SOD1 gene (Al-Chalabi et al. 1998; Eisen et al., 2008; Borel et al., 2016). Research suggests that conformational instability, misfolding, and some degree of aggregation is responsible for mutant SOD1 protein acquiring neurotoxicity (Prudencio et al., 2009). Misfolded SOD1 inclusions were identified in different glial cells of sALS and fALS patients (Forsberg et al., 2011) and selective deletion of mutant SOD1 expression in astrocytes retarded disease progression in a mouse model (Yamanaka et al., 2008). Astrocytes from both sALS and fALS patients, and from the SOD1(G93A) rodent model, are toxic to MNs (Diaz-Amarilla et al., 2011; Meyer et al., 2014) and these cells, with a reactive profile, were present in the primary motor cortex and gray matter from ALS cases (Kamo et al., 1987; Nagy et al., 1994).

MicroRNAs are altered in neurodegenerative diseases e.g., Alzheimer's disease, Parkinson's disease, and Huntington's disease and may serve as markers of disease and response to therapeutic interventions. Early sensitive biomarkers would assist in the early diagnosis in family members at risk of developing ALS and may help in genetic counseling (Benatar et al., 2016). The findings from the articles reviewed herein have indicated dysregulated levels of miRNA expression in the brain, spinal cords, MNs of spinal cord and brainstem,

and hypoglossal, facial, and red motor nuclei of ALS animal models. A large number of miRNAs were upregulated whereas a smaller number were downregulated (**Table 1**). Among the miRNAs found to be upregulated in two or more of the studies by RT-PCR analysis were miR-21, miR-155, miR-125b, miR-146a, miR-124, miR-9, and miR-19b, while those downregulated in two of the studies included miR-146a, miR-29, miR-9, miR-124, and miR-125b. A change of direction in miRNA expression occurred in some tissues when compared (e.g., miR-29b-3p in cerebellum and spinal cord of wobbler mice at 40 days), or at different disease stages (e.g., miR-200a in spinal cord of SOD1(G93A) mice at 95 days *vs.* 108 and 112 days). In the latter case, measurement of such miRNAs would provide important information on the extent of disease progression. Furthermore, suppression of miR-129-5p resulted in increased lifespan, improved muscle strength, reduced NMJ degeneration, and tended to improve MN survival in the SOD1(G93A) mouse model. Suppression of miR-155 was also associated with increased lifespan, while lowering of miR-29a tended to improve lifespan in males and increase muscle strength in SOD1(G93A) mice. Overexpression of members of miR-17~92 cluster improved MN survival in SOD1(G93A) mice and increased lifespan. Moreover, treatment with an artificial miRNA designed to target hSOD1, while not a naturally occurring miRNA that may have a role in disease progression (e.g., in the study by Borel et al. (2016), it was engineered on the backbone of cellular miR-155), was shown to be effective in extending survival in SOD1(G93A) mice (Borel et al., 2016) and also significantly silenced SOD1 expression of MNs in male monkeys (Borel et al., 2016, 2018). From the SOD1(G93A) mouse studies reviewed herein, a small number of miRNAs were dysregulated at the presymptomatic stage e,g., miR-206 and miR-155 both upregulated, while a large number were dysregulated in the early symptomatic and late stage of disease (**Table 1**). It seems plausible that the miRNA changes found in the presymptomatic stage could be contributing to the initiation of the disease, while those occurring in the early symptomatic and late stage could be as a consequence of the disease process itself. Notably, many of the positive findings identified by modifying miRNA levels by intracerebroventricular or intrathecal treatment with agomir or antagomir (**Table 2**) were achieved by administration at the presymptomatic stage. There is a need for further studies to be performed on modifying miRNA levels in SOD1(G93A) mice at the presymptomatic stage and to compare using the same animal model with miRNA levels modified at the symptomatic stage. Interestingly, both the studies by Borel et al. (2016) and Stoica et al. (2016) that showed an amelioration of the disease process by suppressing hSOD1 had administered an artificial miRNA based on the miR-155 sequence to SOD1(G93A) mice in the presymptomatic stage. MiR-155 could be an important contender for future therapeutic manipulation. Downstream effects of miRNA dysregulation could be important in initiating the disease process. For instance, Tung et al. (2019) showed downregulation of miR-17 in lumbar spinal cord MNs at 80 days and increased expression of one of its targets, phosphatase and tensin homologue (PTEN), in MNs at 100 days. PTEN has been linked to the pathogenesis of neurodegenerative disorders including Alzheimer's disease, Parkinson's disease and ALS (Ismail et al., 2012).

With regard to human studies, Figueroa-Romero et al. (2016) identified 90 mature differentially expressed miRNAs in postmortem spinal cord tissue from 12 sALS compared to 12 control subjects, among which nearly all were decreased and only miR-155 and miR-142-5p were increased. Similarly, miR-155 and miR-142-5p were increased in the spinal cord of the SOD1(G93A) mouse model. MiR-125b and miR-29b were downregulated in the postmortem spinal cord tissue of sALS patients. MiR-29b-3p was downregulated in spinal cord at 40 days in wobbler mice. However, miR-125b was upregulated in spinal cord at symptomatic stage (12–14

Review

Reference	Animal model, gender	Sample	Stage of disease	MiRNA analysis method	Upregulation of miRNAs	Downregulation of miRNAs
Spinal cord of SOD1(G93A) mice						
Loffreda et al., 2020	SOD1(G93A) mice, female	Lumbar spinal cord	Presymptomatic, 10 wk; early symptomatic 15 wk, end stage 22 wk	RT-PCR	miR-206	
Loffreda et al., 2020	SOD1(G93A) mice, female	Lumbar spinal cord	Early symptomatic 15 wk	RT-PCR	miR-129-5p, miR-200c	
Tung et al., 2019	SOD1(G93A) mice	Lumbar spinal cord MNs	80 d	RT-PCR		miR-17
Tung et al., 2019	SOD1(G93A) mice	Lumbar spinal cord MNs	100 d	RT-PCR		miR-17, miR-18a, miR-20a
Zhou et al., 2018	SOD1(G93A) mice	Spinal cord	95, 108, 122 d	RT-PCR	miR-219, miR-21, miR-181a	miR-146a, miR-22, miR-26b, miR-34a, miR-320
Zhou et al., 2018	SOD1(G93A) mice	Spinal cord	95 d	RT-PCR	miR-200a, miR-124	
Zhou et al., 2018	SOD1(G93A) mice	Spinal cord	108, 122 d	RT-PCR		miR-200a, miR-124
Cunha et al., 2018	SOD1(G93A) mice, male	Ventral horn of spinal cord	Presymptomatic 4–6 wk	RT-PCR	miR-155	
Cunha et al., 2018	SOD1(G93A) mice, male	Ventral horn of spinal cord	Symptomatic 12–14 wk	RT-PCR	miR-155, miR-125b, miR-146a, miR-21, miR-124	
Hoye et al., 2017	SOD1(G93A) mice	MNs of spinal cord and brainstem	63 d	RT-PCR	miR-218-5p, miR-218-2-3p, miR-138, miR-133a, miR-1193	
Hoye et al., 2017	SOD1(G93A) mice	Spinal cord	126 d	RT-PCR		miR-218-5p, miR-138
Parisi et al., 2016	SOD1(G93A) mice	Lumbar spinal cord	End stage ~23 wk	RT-PCR	miR-125b	
Marcuzzo et al., 2015	SOD1(G93A) mice	Whole spinal cord	Late stage 18 wk	RT-PCR	miR-19a, miR-19b	miR-9, miR-124a
Dobrowolny et al., 2015	MLC/ SOD1(G93A) mice	Spinal cord	4 mon	RT-PCR		miR-133a, miR-133b, miR-9, miR-29, miR-330, miR-1
Nolan et al., 2014	SOD1(G93A) mice	Lumbar spinal cord	Presymptomatic 70 d Symptomatic 90 d	RT-PCR	miR-29a	
Zhou et al., 2013	SOD1(G93A) mice	Spinal cord	95, 108, 122 d	RT-PCR	miR-9	
Koval et al., 2013	SOD1(G93A) mice	Spinal cord	End stage	Microarray analysis	miR-17, miR-19b, miR-20a, miR-24-2-5p, miR-106a, miR-142-3p, miR-142-5p, miR-146a, miR-146b, miR-155, miR-223, miR-338-3p	
Cortical tissue of SOD1(G93A) mice						
Gomes et al., 2019	SOD1(G93A) mice	Cortical tissue	Presymptomatic 4–6 wk	RT-PCR		miR-146a
Gomes et al., 2019	SOD1(G93A) mice	Cortical tissue	Symptomatic 12–14 wk	RT-PCR		miR-125b, miR-21, miR-146a
Whole brain, brain regions of SOD1(G93A) mice						
Marcuzzo et al., 2015	SOD1(G93A) mice	Whole brain	Presymptomatic 8 wk	RT-PCR		miR-19a
Marcuzzo et al., 2015	SOD1(G93A) mice	Whole brain	Late stage 18 wk	RT-PCR	miR-9, miR-124a, miR-19a, miR-19b	
Marcuzzo et al., 2015	SOD1(G93A) mice	SVZ, primary motor cortex, hippocampus, brainstem MN	Late stage 18 wk	RT-PCR	miR-124a	
Marcuzzo et al., 2015	SOD1(G93A) mice	SVZ, hippocampus	Late stage 18 wk	RT-PCR		miR-9, miR-125b
Marcuzzo et al., 2015	SOD1(G93A) mice	Primary motor cortex, brainstem MN	Late stage 18 wk	RT-PCR	miR-9	miR-19b
Marcuzzo et al., 2015	SOD1(G93A) mice	Hippocampus, brainstem MN	Late stage 18 wk	RT-PCR		miR-19a
Marcuzzo et al., 2015	SOD1(G93A) mice	Primary motor cortex	Late stage 18 wk	RT-PCR	miR-19a, miR-125b	
Marcuzzo et al., 2015	SOD1(G93A) mice	Hippocampus	Late stage 18 wk	RT-PCR	miR-19b	
Marcuzzo et al., 2015	SOD1(G93A) mice	SVZ	Late stage 18 wk	RT-PCR		miR-219
Spinal cord of wobbler mice						
Klatt et al., 2019	Wobbler mice	Spinal cord	0 d	RT-PCR	miR-29b-3p	
Klatt et al., 2019	Wobbler mice	Spinal cord	40 d	RT-PCR		miR-29b-3p
Cerebellum of wobbler mice						
Klatt et al., 2019	Wobbler mice	Cerebellum	0 d	RT-PCR		miR-29b-3p
Klatt et al., 2019	Wobbler mice	Cerebellum	40 d	RT-PCR	miR-29b-3p	

Expression levels of miRNAs in amyotrophic lateral sclerosis (ALS) animals compared to control animals. MN: Motor neuron; RT-PCR: real-time quantitative polymerase chain reaction; SVZ: subventricular zone.

Table 2 | Alterations in SOD1(G93A) animal models of amyotrophic lateral sclerosis following overexpression/suppression of specific miRNAs or silencing of hSOD1

Overexpression of miRNA	Suppression of a specific miRNA or hSOD1	Animal model, gender	Route of administration, age of animals	Improved body weight gain	Increased lifespan	Improved muscle strength	Improved MN survival	Counteracted NMJ degeneration	Reference
	miR-129-5p	SOD1(G93A) mice, males and females	i.c.v., 80 d of age, early symptomatic		√	√	Trend shown in lumbar spinal cord	√	Loffreda et al., 2020
miR-17~92		SOD1(G93A) mice	i.t., 60 d of age		√		√		Tung et al., 2019
	miR-155	SOD1(G93A) mice	i.p., 82 d of age; i.c.v., 90 d		√ √				Butovsky et al., 2015
	miR-29a	SOD1(G93A) mice, males and females	i.c.v., 70 of age		Trend in males, but not in females	Trend shown in males and females			Nolan et al., 2014
	miR-155	SOD1(G93A) mice	i.c.v. + i.p., 60 d of age		√				Koval et al., 2013
	hSOD1	SOD1(G93A) mice	into tongue, intrapleural space, 60 d of age	√	√	√			Keeler et al., 2019
	hSOD1	SOD1(G93A) rats	i.t., 65 d of age			√			Hoye et al., 2017
	hSOD1	SOD1(G93A) mice	i.c.v., 0–1 d of age		√		√		Stoica et al., 2016
	hSOD1	SOD1(G93A) mice	i.v., 56–68 d of age		√	√			Borel et al., 2016

√ indicates this was observed in the study; in Borel et al. (2016) the miR-SOD1 was designed based on the backbone of cellular miR-155; in Stoica et al. (2016) the amiR-SOD1 targeted the coding sequence of the human *SOD1* gene and used the endogenous murine miR-155 flanking sequences. i.c.v.: intracerebroventricular; i.p.: intraperitoneal; i.t.: intrathecal; i.v.: intravenous; miRNA: microRNA; MN: motor neuron; NMJ: neuromuscular junction; SOD1: Cu/Zn superoxide dismutase 1.

weeks) and end stage (~23 weeks) of SOD1(G93A) mice. Other miRNAs downregulated in postmortem spinal cord tissue from sALS patients included let-7e, miR-140-3p, miR-133b, miR-148b-5p, and miR-577 (Figueroa-Romero et al., 2016). Also, Koval et al. (2013) observed that miR-243-2*, miR-142-3p, miR-142-5p, miR-146a, miR-146b, and miR-155 were upregulated in postmortem spinal cord samples from 16 ALS patients compared to 12 control subjects, and showed that miR-155 was upregulated in 11 sALS and 5 fALS patients (1.7× increase for both compared to controls). Other studies on miRNAs in postmortem spinal cords were performed with much smaller numbers of sALS patients and control subjects (Campos-Melo et al., 2013; Ishtiaq et al., 2014). Wakabayashi et al. (2014) found that 91 miRNAs were upregulated and 233 downregulated in postmortem cerebral cortex samples from 6 sALS compared to 4 control subjects. MiR-494 (+4.99-fold change) was the most highly differentially upregulated miRNA, followed in order by miR-4257, miR-24-3p, miR-4299, and miR-1973 as the top five up-regulated miRNAs, whereas miR-4740-5p (+0.19-fold change), miR-1290, miR-3619-3p, miR-1246, and miR-3180-3p were the top five downregulated miRNAs. None of these miRNAs were dysregulated in cortical tissue samples from SOD1(G93A) mice in the articles reviewed. Thus, although there have been few studies on miRNA expression in postmortem spinal cord and brain samples of sALS and fALS patients to compare with, there does appear to be some similarities of miRNA expression in spinal cord samples from ALS mouse models. As the *C9orf72* gene is the most prevalent mutated gene among ALS patients, it would be relevant to determine miRNA expression of spinal cord and brain samples in the FVB-C9orf72 BAC transgenic mouse model of ALS. In addition, miRNA expression should be examined in the BSSG-treated mouse model of sALS. Interestingly, ALS-type pathological changes occurred in the brain and spinal cord of vervet monkeys (Chlorocebus sabaeus) fed the cyanotoxin β-N-methylamino-L-alanine and may serve as a nonhuman primate model of ALS that better matches the human patient population (Davis et al., 2020).

Attention was drawn to possible explanations for a difference in findings in C9orf72 mice between the studies of Liu et al. (2016) and Mordes et al. (2020). One possible explanation was the relatively small number of animals in the study by Liu et al. (2016). In fact, many of the reviewed studies had employed small-sized groups of animals (~10–12 or less per group). Future studies that are performed with much larger cohorts of animals would be more informative and the findings less likely to be refuted. Furthermore, most of the studies reviewed did not report the gender of the animals used, or if they had, it was only males or females. Clearly studies need to be performed with approximately equal and a sufficient number of male and female animals, so that the findings can be statistically analyzed in both. Gender differences in the composition of groups could constitute a confounding factor and statistical analyses of data should be corrected by performing multiple comparisons. Also, normalization of miRNA data should be performed using normalizing miRNA species, but this was only reported in eight of the studies reviewed. It is not clear whether it was included in the remaining studies.

Novel therapies aimed at silencing SOD1 include inhibitory short hairpin RNA, artificial miRNA, ASOs, and virally delivered silencing elements. In the studies reviewed, an artificial miRNA targeting hSOD1 delivered i.t. by ASO or i.v. by AAVrh10 to ALS mice resulted in increased lifespan, and improved muscle strength. These changes were also seen using an AAV9 artificial miRNA against hSOD1 delivered i.c.v. (Table 2). Recently the US Food and Drug Administration approved an ASO therapeutic agent, Nusinersen, for spinal muscular atrophy. This provides a successful model of intervention in other MN diseases, including ALS (Parente and Corti, 2018). SOD1 ASOs have been shown to be safe in humans (Miller et al., 2013) and a clinical trial is currently underway to treat SOD1-related ALS using a second-generation ASO, Tofersen (BIIB067, Ionis-SOD1Rx, ASO1) (ClinicalTrials.gov., 2020

Review

https://clinicaltrials.gov/ct2/show/NCT02623699; Alzoforum, 2020 https://www.alzforum.org/therapeutics/tofersen). A newly emerging and promising therapeutic modality is gene-editing. Both CRISPR nucleases (Gaj et al., 2017) and CRISPR base editors (Lim et al., 2020) have been used to target SOD1 as a treatment of ALS in a mouse model of ALS, and improved motor function and prolonged survival.

In conclusion, genetic animal models of ALS show some of the changes in miRNA expression that have been reported in the spinal cord of sALS and fALS patients. They have proven to be useful in testing possible therapies for ALS e.g., human SOD1 mRNA was decreased in spinal cords of SOD1(G93A) mice with approximately 75% reduction of SOD1 following a single intraventricular injection of ASO 1 or ASO 2. Similar dose-dependent reductions in human SOD1 mRNA were achieved in SOD1(G93A) rats with ASO 1 and ASO 2 (McCampbell et al., 2018). This review underlies the importance and need for further studies with ALS animal models, especially nonhuman primates, specifically testing ASOs or AAV vectors carrying miRNAs to target human SOD1 or other genes to provide a more effective means of treating ALS and slowing its progression, and which hopefully may be successfully translated to human ALS patients.

References

Abe K, Aoki M, Tsuji S, Itoyama Y, Sobue G, Togo M, Hamada C, Tanaka M, Akimoto M, Nakamura K, Takahashi F, Kondo K, Yoshino H (2017) Safety and efficacy of edaravone in well defined patients with amyotrophic lateral sclerosis: a randomised, double-blind, placebo-controlled trial. Lancet Neurol 16:505-512.

Achi EY, Rudnicki SA (2012) ALS and frontotemporal dysfunction: a review. Neurol Res Int 2012:806306.

Ajroud-Driss S, Siddique T (2015) Sporadic and hereditary amyotrophic lateral sclerosis (ALS). Biochim Biophys Acta 1852:679-684.

Al-Chalabi A, Andersen PM, Chioza B, Shaw C, Sham PC, Robberecht W, Matthijs G, Camu W, Marklund SL, Forsgren L, Rouleau G, Laing NG, Hurse PV, Siddique T, Leigh PN, Powell JF (1998) Recessive amyotrophic lateral sclerosis families with the D90A SOD1 mutation share a common founder: evidence for a linked protective factor. Hum Mol Genet 7:2045-2050.

Al-Chalabi A, Hardiman O (2013) The epidemiology of ALS: a conspiracy of genes, environment and time. Nat Rev Neurol 9:617-628.

Al-Chalabi A, Hardiman O, Kiernan MC, Chiò A, Rix-Brooks B, van den Berg LH (2016) Amyotrophic lateral sclerosis: moving towards a new classification system. Lancet Neurol 15:1182-1194.

Alzoforum (2020) Therapeutics Tofersen. https://www.alzforum.org/therapeutics/tofersen. Accessed December 7, 2020.

Arnold ES, Ling SC, Huelga SC, Lagier-Tourenne C, Polymenidou M, Ditsworth D, Kordasiewicz HB, McAlonis-Downes M, Platoshyn O, Parone PA, Da Cruz S, Clutario KM, Swing D, Tessarollo L, Marsala M, Shaw CE, Yeo GW, Cleveland DW (2013) ALS-linked TDP-43 mutations produce aberrant RNA slicing and adult-onset motor neuron disease without aggregation or loss of nuclear TDP-43. Proc Natl Acad Sci U S A 110:E736-745.

Benatar M, Stanislaw C, Reyes E, Hussain S, Cooley A, Fernandez MC, Dauphin DD, Michon SC, Andersen PM, Wuu J (2016) Presymptomatic ALS genetic counseling and testing: experience and recommendations. Neurology 86: 2295-2302.

Benigni M, Ricci C, Jones AR, Giannini F, Al-Chalabi A, Battistini S (2016) Identification of miRNAs as potential biomarkers in cerebrospinal fluid from amyotrophic lateral sclerosis patients. Neuromol Med 18:551-560.

Boillee S, Peschanski M, Junier MP (2003) The wobbler mouse: a neurodegeneration jigsaw puzzle. Mol Neurobiol 28:65-106.

Boone DL, Turer EE, Lee EG, Ahmad RC, Wheeler MT, Tsui C, Hurley P, Chien M, Chai S, Hitotsumatsu O, McNally E, Pickart C, Ma A (2004) The ubiquitin-modifying enzyme A20 is required for termination of Toll-like receptor responses. Nat Immunol 5:1052-1060.

Borel F, Gernoux G, Cardozo B, Metterville JP, Toro Cabrera GC, Song L, Su Q, Gao GP, Elmallah MK, Brown RH Jr, Mueller C (2016) Therapeutic rAAVrh10 mediated SOD1 silencing in adult SOD1(G93A) mice and nonhuman primates. Hum Gene Ther 27:19-31.

Borel F, Gernoux G, Sun H, Stock R, Blackwood M, Brown RH Jr, Mueller C (2018) Safe and effective superoxide dismutase 1 silencing using artificial microRNA in macaques. Sci Trans Med 10:eaau6414.

Brites D, Vaz AR (2014) Microglia centered pathogenesis in ALS: insights in cell interconnectivity. Front Cell Neurosci 8:117.

Brown RH, Al-Chalabi A (2017) Amyotrophic lateral sclerosis. New Eng J Med 377:162-172.

Bruijn LI, Miller TM, Cleveland DW (2001) Unraveling the mechanisms involved in motor neuron degeneration in ALS. Annu Rev Neurosci 27:723-749.

Bucchia M, Ramirez A, Parente V, Simone C, Nizzardo M, Magri F, Dametti S, Corti S (2015) Therapeutic development in amyotrophic lateral sclerosis. Clin Ther 37:668-680.

Buratti E, De Conti L, Stuani C, Romano M, Baralle M, Baralle F (2010) Nuclear factor TDP-43 can affect selected microRNA levels. FEBS J 277:2268-2281.

Butovsky O, Siddiqui S, Gabriely G, Lanser AJ, Dake B, Murugaiyan G, Doykan CE, Wu PM, Gali RR, Iyer LK, Lawson R, Berry J, Krichevsky AM, Cudkowicz ME, Weiner HL (2012) Modulating inflammatory monocytes with a unique microRNA gene signature ameliorates murine ALS. J Clin Invest 122:3063-3087.

Butovsky O, Jedrychowski MP, Cialic R, Krasemann S, Murugaiyan G, Fanek Z, Greco DJ, Wu PM, Doykan CE, Kiner O, Lawson RJ, Frosch MP, Pochet N, Fatimy RE, Krichevsky AM, Gygi SP, Lassmann H, Berry J, Cudkowicz ME, Weiner HL (2015) Targeting miR-155 restores abnormal microglia and attenuates disease in SOD1 mice. Ann Neurol 77:75-99.

Cabellero-Hernandez D, Toscano MG, Cejudo-Guillen M, Garcia-Martin ML, Lopez S, Franco JM, Quintana FJ, Roodveldt C, Pozo D (2016) The 'omics' of amyotrophic lateral sclerosis. Trends Mol Med 22:53-67.

Campos-Melo D, Droppelmann CA, He Z, Volkening K, Strong MJ (2013) Altered microRNA profile in amyotrophic lateral sclerosis: a role in the regulation of NFL mRNA levels. Mol Brain 6:26.

Chia R, Chiò A, Traynor BJ (2018) Novel genes associated with amyotrophic lateral sclerosis: diagnostic and clinical implications. Lancet Neurol 17:94-102.

ClinicalTrials.gov. (2020) An efficacy, safety, tolerability, pharmacokinetics and pharmacodynamics study of BIIB067 in adults with inherited amyotrophic lateral sclerosis (ALS) (VALOR) (Part C). https://clinicaltrials.gov/ct2/show/NCT02623699. Accessed December 7, 2020.

Coornaert B, Carpentier I, Beyaert R (2009) A20: the central gatekeeper in inflammation and immunity. J Biol Chem 284:8217-8221.

Cunha C, Gomes C, Vaz AR, Brites D (2016) Exploring new inflammatory biomarkers and pathways during LPS-induced M1 polarization. Mediat Inflamm 2016:6986175.

Cunha C, Santos C, Gomes C, Fernandes A, Correia AM, Sebastião AM, Vaz AR, Brites D (2018) Downregulated glia interplay and increased miRNA-155 as promising markers to track ALS at an early stage. Mol Neurobiol 55:4207-4224.

Dahlke C, Saberi D, Ott B, Brand-Saberi B, Schmitt-John T, Theiss C (2015) Inflammation and neuronal death in the motor cortex of the wobbler mouse, an ALS animal model. J Neuroinflamm 12:215.

Davis DA, Cox PA, Banack SA, Lecusay PD, Garamszegi SP, HaganMJ, Powell JT, Metcalf JS, Palmour RM, Beierschmitt A, Bradley WG, Mash DC (2020) L-Serine reduces spinal cord pathology in a vervet model of preclinical ALS/MND. J Neuropathol Exp Neurol 79:393-406.

De Felice B, Annunziata A, Fiorentino G, Borra M, Biffali E, Coppola C, Cotrufo R, Brettschneider J, Giordana ML, Dalmay T, Wheeler G, D'Alessandro R (2014) miR-338-3p is over-expressed in blood, CSF, serum and spinal cord from sporadic amyotrophic lateral sclerosis patients. Neurogenetics15:243-253.

DeJesus-Hernandez M, Mackenzie IR, Boeve BF, Boxer AL, Baker M, Rutherford NJ, Nicholson AM, Finch NA, Flynn H, Adamson J, Kouri N, Wojtas A, Sengdy P, Hsiung GY, Karydas A, Seeley WW, Josephs KA, Coppola G, Geschwind DH, Wszolek ZK, et al. (2011) Expanded GGGGCC hexanucleotide repeat in non-coding region of C9ORF72 causes chromosome 9p-linked FTD and ALS. Neuron 72:245-256.

Dennis JS, Citron BA (2009) Wobbler mice modeling motor neuron disease display elevated transactive response DNA binding protein. Neuroscience 158:745-750.

Diaz-Amarilla P, Olivera-Bravo S, Trias E, Cragnolini A, Martínez-Palma L, Cassina P, Beckman J, Barbeito L (2011) Phenotypically aberrant astrocytes that promote motoneuron damage in a model of inherited amyotrophic lateral sclerosis. Proc Natl Acad Sci U S A 108:18126-18131.

Dobrowolny G, Bernardini C, Martini M, Baranzini M, Barba M, Musarò A (2015) Muscle expression of SOD1(G93A) modulates microRNA and mRNA transcription pattern associated with the myelination process in the spinal cord of transgenic mice. Front Cell Neurosci 9:463.

Droppelmann CA, Campos-Melo D, Ishtiaq M, Volkening K, Strong MJ (2014) RNA metabolism in ALS: when normal processes become pathological. Amyotroph Lateral Scler Frontotemporal Degener 15:321-336.

Duchen LW, Strich SJ (1968) An hereditary motor neurone disease with progressive denervation of muscle in the mouse: the mutant 'wobbler'. J Neurol Neurosurg Psychiatry 31:535-542.

Eisen A, Mezei MM, Stewart HG, Fabros M, Gibson G, Andersen PM (2008) SOD1 gene mutations in ALS patients from British Columbia, Canada: clinical features, neurophysiology and ethical issues in management. Amyotroph Lateral Scler 9:108-119.

Eitan C, Hornstein E (2016) Vulnerability of microRNA biogenesis in FTD-ALS. Brain Res 1647:105-111.

Emde A, Eitan C, Liou LL, Libby RT, Rivkin N, Magen I, Reichenstein I, Oppenheim H, Eilam R, Silvestroni A, Alajajian B, Ben-Dov IZ, Aebischer J, Savidor A, Levin Y, Sons R, Hammond SM, Ravits JM, Möller T, Hornstein E (2015) Dysregulated miRNA biogenesis downstream of cellular stress and ALS-causing mutations: a new mechanism for ALS. EMBO J 34:2633-2651.

Falconer DS (1956) Wobbler mouse. News Lett 15:23.

Ferraiuolo L, Kirby J, Grierson AJ, Sendtner M, Shaw PJ (2001) Molecular pathways of motor neuron injury in amyotrophic lateral sclerosis. Nat Rev Neurol 7:616-630.

Figueroa-Romero C, Hur J, Lunn JS, Paez-Colasante X, Bender DE, Yung R, Sakowski SA, Feldman EL (2016) Expression of microRNAs in human post-mortem amyotrophic lateral sclerosis spinal cords provides insight into disease mechanisms. Mol Cell Nerosci 71:34-45.

Forsberg K, Andersen PM, Marklund SL, Brännström T (2011) Glial nuclear aggregates of superoxide dismutase-1 are regularly present in patients with amyotrophic lateral sclerosis. Acta Neuropathol 121:623-634.

Freischmidt A, Müller K, Zondler L, Weydt P, Mayer B, von Arnim CA, Hübers A, Dorst J, Otto M, Holzmann K, Ludolph AC, Danzer KM, Weishaupt JH (2015) Serum microRNAs in sporadic amyotrophic lateral sclerosis. Neurobiol Aging 36:2660.e15-20.

Gaj T, Ojala DS, Ekman FK, Byrne LC, Limsirichai P, Schaffer DV (2017) In vivo genome editing improves motor function and extends survival in a mouse model of ALS. Sci Adv 3:eaar3952.

Gascon E, Gao FB (2014) The emerging roles of microRNAs in the pathogenesis of frontotemporal dementia-amyotrophic lateral sclerosis (FTD-ALS) spectrum disorders. J Neurogenet 28:30-40.

Gomes C, Cunha C, Nascimento F, Ribeiro JA, Vaz AR, Brites D (2019) Cortical neurotoxic astrocytes with early ALS pathology and miR-146a deficit replicate gliosis markers of symptomatic SOD1G93A mouse model. Mol Neurobiol 56:2137-2158.

Goodall EF, Heath PR, Bandmann O, Kirby J, Shaw PJ (2013) Neuronal dark matter: the emerging role of microRNAs in neurodegeneration. Front Cell Neurosci 7:178.

Gruzman A, Wood WL, Alpert E, Prasad MD, Miller RG, Rothstein JD, Bowser R, Hamilton R, Wood TD, Cleveland DW, Lingappa VR, Liu J (2007) Common molecular signature in SOD1 for both sporadic and familial amyotrophic lateral sclerosis. Proc Natl Acad Sci U S A 104:12524-12529.

Guil S, Cáceres JF (2007) The multi-functional RNA-binding protein hnRNP A1 is required for processing of miR-18a. Nat Struct Mol Biol 14:591-596.

Gurney ME (1994) Transgenic-mouse model of amyotrophic lateral sclerosis. New Eng J Med 331:1721-1722.

Gurney ME (1997) The use of transgenic mouse models of amyotrophic lateral sclerosis in preclinical drug studies. J Neurol Sci 152 Suppl 1:S67-73.

Haeusler AR, Donnelly CJ, Periz G, Simko EA, Shaw PG, Kim MS, Maragakis NJ, Troncoso JC, Pandey A, Sattler R, Rothstein JD, Wang J (2014) C9orf72v nucleotide repeat structures initiate molecular cascades of disease. Nature 507:195-200.

Haramati S, Chapnik E, Sztainberg Y, Eilam R, Zwang R, Gershoni N, McGlinn E, Heiser PW, Wills AM, Wirguin I, Rubin LL, Misawa H, Tabin CJ, Brown R Jr, Chen A, Hornstein E (2010) miRNA malfunction causes spinal motor neuron disease. Proc Natl Acad Sci U S A 107:13111-13116.

Hou Q, Ruan H, Gilbert J, Wang G, Ma Q, Yao WD, Man HY (2015) MicroRNA miR124 is required for the expression of homeostatic synaptic plasticity. Nat Commun 6:10045.

Howland DS, Liu J, She Y, Goad B, Maragakis NJ, Kim B, Erickson J, Kulik J, DeVito L, Psaltis G, DeGennaro LJ, Cleveland DW, Rothstein JD (2002) Focal loss of glutamate transporter EAAT2 in a transgenic rat model of SOD1 mutant-mediated amyotrophic lateral sclerosis (ALS). Proc Natl Acad Sci U S A 99: 1604-1609.

Hoye ML, Koval ED, Wegener AJ, Hyman TS, Yang C, O'Brien DR, Miller RL, Cole T, Schoch KM, Shen T, Kunikata T, Richard JP, Gutmann DH, Maragakis NJ, Kordasiewicz HB, Dougherty JD, Miller TM (2017) MicroRNA profiling reveals marker of motor neuron disease in ALS models. J Neurosci 37:5574-5586.

Ishtiaq M, Campos-Melo D, Volkening K, Strong MJ (2014) Analysis of novel NEFL mRNA targeting microRNAs in amyotrophic lateral sclerosis. PLoS One 9:e85653.

Ismail A, Ning K, Al-Hayani A, Sharrack B, Azzouz M (2012) PTEN: a molecular target for neurodegenerative disorders. Trans Neurosci 3:132-142.

Kabashi E, Valdmanis PN, Dion P, Spiegelman D, McConkey BJ, Vande Velde C, Bouchard JP, Lacomblez L, Pochigaeva K, Salachas F, Pradat PF, Camu W, Meininger V, Dupre N, Rouleau GA (2008) TARDBP mutations in individuals with sporadic and familial amyotrophic lateral sclerosis. Nat Genet 40:572-574.

Kamo H, Haebara H, Akiguchi I, Kameyama M, Kimura H, McGeer PL (1987) A distinctive distribution of reactive astroglia in the precentral cortex in amyotrophic lateral sclerosis. Acta Neuropathol 74:33-38.

Kanning KC, Kaplan A, Henderson CE (2010) Motor neuron diversity in development and disease. Annu Rev Neurosci 33:409-440.

Kawahara Y, Mieda-Sato A (2012) TDP-43 promotes microRNA biogenesis as a component of Drosha and Dicer complexes. Proc Natl Acad Sci U S A 109:3347-3352.

Keeler AM, Zieger M, Semple C, Pucci L, Veinbachs A, Brown RH Jr, Mueller C, ElMallah MK (2019) Intralingual and intrapleural AAV gene therapy prolongs survival in SOD1 ALS mouse model. Mol Ther Methods Clin Dev 17:246-257.

Kiernan MC, Vucic S, Cheah BC, Turner MR, Eisen A, Hardiman O, Burrell JR, Zoing MC (2011) Amyotrophic lateral sclerosis. Lancet 377:942-955.

Klatt CL, Theis V, Hahn S, Theiss C, Matschke V (2019) Deregulated miR-29b-3p correlated with tissue-specific activation of intrinsic apoptosis in an animal model of amyotrophic lateral sclerosis. Cells 8:1077.

Koval ED, Shaner C, Zhang P, du Maine X, Fischer K, Tay J, Chau BN, Wu GF, Miller TM (2013) Method for widespread microRNA-155 inhibition prolongs survival in ALS-model mice. Hum Mol Genet 22:4127-4135.

Kwiatkowski Jr. TJ, Bosco DA, Leclerc AL, Tamrazian E, Vanderburg CR, Russ C, Davis A, Gilchrist J, Kasarskis EJ, Munsat T, Valdmanis P, Rouleau GA, Hosler BA, Cortelli P, de Jong PJ, Yoshinaga Y, Haines JL, Pericak-Vance MA, Yan J, Ticozzi N, et al. (2009) Mutations in the FUS/TLS gene on chromosome 16 cause familial amyotrophic lateral sclerosis. Science 323:1205-1208.

Kye MJ, Gonçalves Ido C (2014) The role of miRNA in motor neuron disease. Front Cell Neurosci 8:15.

Le MT, Xie H, Zhou B, Chia PH, Rizk P, Um M, Udolph G, Yang H, Lim B, Lodish HF (2009) MicroRNA-125b promotes neural differentiation in human cells by repressing multiple targets. Mol Cell Biol 29:5290-5305.

Lim CK, Gapinske M, Brooks AK, Woods WS, Powell JE, Zeballos C MA, Winter J, Perez-Pinera P, Gaj T (2020) Treatment of a mouse model of ALS by in vivo base editing. Mol Ther 28:1177-1189.

Liu Y, Pattamatta A, Zu T, Reid T, Bardhi O, Borchelt DR, Yachnis AT, Ranum LP (2016) C9orf72 BAC mouse model with motor deficits and neurodegenerative features of ALD/FTD. Neuron 90:521-534.

Loffreda A, Nizzardo M, Arosio A, Ruepp MD, Calogero RA, Volinia S, Galasso M, Bendotti C, Ferrarese C, Lunetta C, Rizzuti M, Ronchi AE, Mühlemann O, Tremolizzo L, Corti S, Barabino SML (2020) miR-129-5p: a key factor and therapeutic target in amyotrophic lateral sclerosis. Prog Neurobiol 190:101803.

Lutz C (2018) Mouse models of ALS: past, present and future. Brain Res 1693 (Pt A): 1-10.

Majounie E, Renton AE, Mok K, Dopper EG, Waite A, Rollinson S, Chiò A, Restagno G, Nicolaou N, Simon-Sanchez J, van Swieten JC, Abramzon Y, Johnson JO, Sendtner M, Pamphlett R, Orrell RW, Mead S, Sidle KC, Houlden H, Rohrer JD, et al. (2012) Frequency of the C9orf72 hexanucleotide repeat expansion in patients with amyotrophic lateral sclerosis and frontotemporal dementia: a cross-sectional study. Lancet Neurol 11:323-330.

Marcuzzo S, Zucca I, Mastropietro A, de Rosbo NK, Cavalcante P, Tartari S, Bonanno S, Preite L, Mantegazza R, Bernasconi P (2011) Hind limb muscle atrophy precedes cerebral neuronal degeneration in G93A-SOD1 mouse model of amyotrophic lateral sclerosis: a longitudinal MRI study. Exp Neurol 231:30-37.

Marcuzzo S, Kapetis D, Mantegazza R, Baggi F, Bonanno S, Barzago C, Cavalcante P, Kerlero de Rosbo N, Bernasconi P (2014) Altered miRNA expression is associated with neuronal fate in G93A-SOD1 ependymal stem progenitor cells. Exp Neurol 253:91-101.

Marcuzzo S, Bonanno S, Kapetis D, Barzago C, Cavalcante P, D'Alessandro S, Mantegazza R, Bernasconi P (2015) Up-regulation of neural and cell cycle-related microRNAs in brain of amyotrophic lateral sclerosis mice at late disease stage. Mol Brain 8:5.

Martin LJ (2000) p53 is abnormally elevated and active in the CNS of patients with amyotrophic lateral sclerosis. Neurobiol Dis 7:613-622.

McCampbell A, Cole T, Wegener AJ, Tomassy GS, Setnicka A, Farley BJ, Schoch KM, Hoye ML, Shabsovich M, Sun L, Luo Y, Zhang M, Comfort N, Wang B, Amacker J, Thankamony S, Salzman DW, Cudkowicz M, Graham DL, Bennett CF, et al. (2018) Antisense oligonucleotides extend survival and reverse decrement in muscle response in ALS models. J Clin Invest 128:3558-3567.

McCombe PA, Henderson RD (2011) The role of immune and inflammatory mechanisms in ALS. Curr Mol Med 11:246-254.

Meyer K, Ferraiuolo L, Miranda CJ, Likhite S, McElroy S, Renusch S, Ditsworth D, Lagier-Tourenne C, Smith RA, Ravits J, Burghes AH, Shaw PJ, Cleveland DW, Kolb SJ, Kaspar BK (2014) Direct conversion of patient fibroblasts demonstrates non-cell autonomous toxicity of astrocytes to motor neurons in familial and sporadic ALS. Proc Natl Scad Sci U S A 111:829-834.

Miller RG, Mitchell JD, Moore DH (2012) Riluzole for amyotrophic lateral sclerosis (ALS)/motor neuron disease (MND). Cochrane Database Syst Rev 3: CD001447.

Miller TM, Pestronk A, David W, Rothstein J, Simpson E, Appel SH, Andres PL, Mahoney K, Allred P, Alexander K, Ostrow LW, Schoenfeld D, Macklin EA, Norris DA, Manousakis G, Crisp M, Smith R, Bennett CF, Bishop KM, Cudkowicz ME (2013) An antisense oligonucleotide against SOD1 delivered intrathecally for patients with SOD1 familial amyotrophic lateral sclerosis: a phase 1, randomised, first-in-man study. Lancet Neurol 12:434-442.

Mitchell JC, McGoldrick P, Vance C, Hortobagyi T, Sreedharan J, Rogelj B, Tudor EL, Smith BN, Klasen C, Miller CC, Cooper JD, Greensmith L, Shaw CE (2013) Overexpression of human wild-type FUS causes progressive motor neuron degeneration in age- and dose-dependent fashion. Acta Neuropathol 125: 273-288.

Mitsumoto H, Ferut AL, Kurahashi K, Jacob JM, McQuarrie IG (1990) Impairment of retrograde axonal transport in wobbler mouse motor neuron disease. Muscle Nerve 13:121-126.

Mordes DA, Morrison BM, Ament XH, Cantrell C, Mok J, Eggan P, Xue C, Wang JY, Eggan K, Rothstein JD (2020) Absence of survival and motor deficits in 500 repeat C9ORF72 BAC mice. Neuron 108:775-783.

Morlando M, Dini Modigliani S, Torrelli G, Rosa A, Di Carlo V, Caffarelli E, Bozzoni I (2012) FUS stimulates microRNA biogenesis by facilitating co-transcriptional Drosha recruitment. EMBO J 31:4502-4510.

Moser JM, Bigini P, Schmitt-John T (2013) The wobbler mouse, an ALS animal model. Mol Genet Genomics 288:207-229.

Review

Nagy D, Kato T, Kushner PD (1994) Reactive astrocytes are widespread in the cortical gray matter of amyotrophic lateral sclerosis. J Neurosci Res 38:336-347.

Nardo G, Trolese MC, Tortarolo M, Vallarola A, Freschi M, Pasetto L, Bonetto V, Bendotti C (2016) New insights on the mechanisms of disease course variability in ALS from mutant SOD1 mouse models. Brain Pathol 26:237-247.

Nolan K, Mitchem MR, Jimenez-Mateos EM, Henshall DC, Concannon CG, Prehn JH (2014) Increased expression of microRNA-29a in ALS mice: functional analysis of its inhibition. J Mol Neurosci 53:231-241.

O'Rourke JG, Bogdanik L, Muhammad AK, Gendron TF, Kim KJ, Austin A, Cady J, Liu EY, Zarrow J, Grant S, Ho R, Bell S, Carmona S, Simpkinson M, Lall D, Wu K, Daughrity L, Dickson DW, Harms MB, Petrucelli L, et al. (2015) C9orf72 BAC transgenic mice display typical pathologic features of ALS/FTD. Neuron 88:892-901.

Ott B, Dahlke C, Meller K, Napirei M, Schmitt-John T, Brand-Saberi B, Theiss C, Saberi D (2015) Implementation of a manual for working with wobbler mice and criteria for discontinuation of the experiment. Ann Anat 200:118-124.

Paez-Colasante X, Figueroa-Romero C, Sakowski SA, Goutman SA, Feldman EL (2015) Amyotrophic lateral sclerosis: mechanisms and therapeutics in the epigenomic era. Nat Rev Neurol 11:266-279.

Palmisano R, Golfi P, Heimann P, Shaw C, Troakes C, Schmitt-John T, Bartsch JW (2011) Endosomal accumulation of APP in wobbler mouse motor neurons reflects impaired vesicle trafficking: implications for human motor neuron disease. BMC Neurosci 12:24.

Parente V, Corti S (2018) Advances in spinal muscular atrophy therapeutics. Ther Adv Neurol Disord 11:1756285618754501.

Parisi C, Napoli G, Amadio S, Spalloni A, Apolloni S, Longone P, Volonté C (2016) MicroRNA-125b regulates microglia death in ALS. Cell Death Diff 23: 531-541.

Pathak S, Grillo AR, Scarpa M, Brun P, D'Incà R, Nai L, Banerjee A, Cavallo D, Barzon L, Palù G, Sturniolo GC, Buda A, Castagliuolo I (2015) MiR-155 modulates the inflammatory phenotype of intestinal myofibroblasts by targeting SOCS1 in ulcerative colitis. Exp Mol Med 47:e164.

Peters OM, Cabrera GT, Tran H, Gendron TF, McKeon JE, Metterville J, Weiss A, Wightman N, Salameh J, Kim J, Sun H, Boylan KB, Dickson D, Kennedy Z, Lin Z, Zhang YJ, Daughrity L, et al. (2015) Human C9ORF72 hexanucleotide expansion reproduces RNA foci and dipeptide repeat proteins but not neurodegeneration in BAC transgenic mice. Neuron 88:902-909.

Philips T, Rothstein JD (2015) Rodent models of amyotrophic lateral sclerosis. Curr Protoc Pharmacol 69:5.67.1-5.67.21.

Ponomarev ED, Veremeyko T, Barteneva N, Krichevsky AM, Weiner HL (2011) MicroRNA-124 promotes microglia quiescence and suppresses EAE by deactivating macrophages via the C/EBP-α-PU.1 pathway. Nat Med 17:64-70.

Ponomarev ED, Veremeyko T, Weiner HL (2013) MicroRNAs are universal regulators of differentiation, activation, and polarization of microglia and macrophages in normal and diseased CNS. Glia 61:91-103.

Prudencio M, Hart PJ, Borchelt DR, Andersen PM (2009) Variation in aggregation propensities among ALS-associated variants of SOD1: correlation to human disease. Hum Mol Genet 18:3217-3226.

Pun S, Santos AF, Saxena S, Xu L, Caroni P (2006) Selective vulnerability and pruning of phasic motoneuron axons in motoneuron disease alleviated by CNTF. Nat Neurosci 9:408-419.

Renton AE, Majounie E, Waite A, Simón-Sánchez J, Rollinson S, Gibbs JR, Schymick JC, Laaksovirta H, van Swieten JC, Myllykangas L, Kalimo H, Paetau A, Abramzon Y, Remes AM, Kaganovich A, Scholz SW, Duckworth J, Ding J, Harmer DW, Hernandez DG, et al. (2011) A hexanucleotide repeat expansion in C9ORF72 is the cause of chromosome 9p21-linked ALS-FTD. Neuron 72:257-268.

Renton AE, Chiò A, Traynor BJ (2014) State of play in amyotrophic lateral sclerosis genetics. Nat Neurosci 17:17-23.

Rocha MC, Pousinha PA, Correia AM, Sebastião AM, Ribeiro JA (2013) Early changes of neuromuscular transmission in the SOD1(G93A) mice model of ALS start long before motor symptoms onset. PLoS One 8:e73846.

Rohm M, May C, Marcus K, Steinbach S, Theis V, Theiss C, Matschke V (2019) The microRNA miR-375-3p and the tumor suppressor NDRG2 are involved in sporadic amyotrophic lateral sclerosis. Cell Physiol Biochem 52: 1412-1426.

Rosen DR, Siddique T, Patterson D, Figlewicz DA, Sapp P, Hentati A, Donaldson D, Goto J, O'Regan JP, Deng HX, Rahmani Z, Krizus A, McKenna-Yasek D, Cayabyab A, Gaston SM, Berger R, Tanzi RE, Halperin JJ, Herzfeldt B, Van Den Bergh R, et al. (1993) Mutations in the Cu/Zn superoxide dismutase gene are associated with familial amyotrophic lateral sclerosis. Nature 362:59-62.

Russell AP, Wada S, Vergani L, Hock MB, Lamon S, Léger B, Ushida T, Cartoni R, Wadley GD, Hespel P, Kralli A, Soraru G, Angelini C, Akimoto T (2013) Disruption of skeletal muscle mitochondrial network genes and miRNAs in amyotrophic lateral sclerosis. Neurobiol Dis 49:107-117.

Russell AP, Ghobrial L, Ngo S, Yerbury J, Zacharewicz E, Chung R, Lamon S (2018) Dysregulation of microRNA biogenesis machinery and microRNA/RNA ratio in skeletal muscle of amyotrophic lateral sclerosis mice. Muscle Nerve 57:838-847.

Saba R, Gushue S, Huzarewich RL, Manguiat K, Medina S, Robertson C, Booth SA (2012) MicroRNA 146a (miR-146a) is over-expressed during prion disease and modulates the innate immune response and the microglial activation state. PLoS One 7:e30832.

Saberi D, Ott B, Dahlke C, Matschke V, Schmitt-John T, Theiss C (2016) The spatiotemporal pattern of degeneration in the cerebellum of the wobbler mouse. J Neuropathol Exp Neur 75:347-357.

Saxena S, Caroni P (2011) Selective neuronal vulnerability in neurodegenerative diseases: from stressor thresholds to degeneration. Neuron 71:35-48.

Schmitt-John T, Drepper C, Mussmann A, Hahn P, Kuhlmann M, Thiel C, Hafner M, Lengeling A, Heimann P, Jones JM, Meisler MH, Jockusch H (2005) Mutation of Vps54 causes motor neuron disease and defective spermiogenesis in the wobbler mouse. Nat Genet 37:1213-1215.

Shaw PJ, Eggett CJ (2000) Molecular factors underlying selective vulnerability of motor neurons to neurodegeneration in amyotrophic lateral sclerosis. J Neurol 247 Suppl 1:117-127.

Sreedharan J, Blair IP, Tripathi VB, Hu X, Vance C, Rogelj B, Ackerley S, Durnall JC, Williams KL, Buratti E, Baralle F, de Belleroche J, Mitchell JD, Leigh PN, Al-Chalabi A, Miller CC, Nicholson G, Shaw CE (2008) TDP-43 mutations in familial and sporadic amyotrophic lateral sclerosis. Science 319:1668-1672.

Stoica LK, Todeasa SH, Cabrera GT, Salameh JS, ElMallah MK, Mueller C, Brown RH Jr, Sena-Esteves M (2016) Adeno-associated virus-delivered artificial microRNA extends survival and delays paralysis in an amyotrophic lateral sclerosis mouse model. Ann Neurol 79:687-700.

Stribl C, Samara A, Trümbach D, Peis R, Neumann M, Fuchs H, Gailus-Durner V, Hrabě de Angelis M, Rathkolb B, Wolf E, Beckers J, Horsch M, Neff F, Kremmer E, Koob S, Reichert AS, Hans W, Rozman J, Klingenspor M, Aichler M, et al. (2014) Mitochondrial dysfunction and decrease in body weight of a transgenic knock-in mouse model for TDP-43. J Biol Chem 289:10769-10784.

Swinnen B, Robberecht W (2014) The phenotypic variability of amyotrophic lateral sclerosis. Nat Rev Neurol 10:661-670.

Tabata RC, Wilson JM, Ly P, Zwiegers P, Kwok D, Van Kampen JM, Cashman N, Shaw CA (2008) Chronic exposure to dietary sterol glucosides is neurotoxic to motor neurons and induces an ALS-PDC phenotype. Neuromolecular Med 10:24-39.

Takahashi I, Hama Y, Matsushima M, Hirotani M, Kano T, Hohzen H, Yabe I, Utsumi J, Sasaki H (2015) Identification of plasma microRNAs as a biomarker of sporadic amyotrophic lateral sclerosis. Mol Brain 8:67.

Tasca E, Pegoraro V, Merico A, Angelini C (2016) Circulating micrornas as biomarkers of muscle differentiation and atrophy in ALS. Clin Neuropathol 35: 22-30.

Taylor JP, Brown RH Jr, Cleveland DW (2016) Decoding ALS: from genes to mechanism. Nature 539:197-206.

Tung YT, Peng KC, Chen YC, Yen YP, Chang M, Thams S, Chen JA (2019) Mir-17~92 confers motor neuron subtype differential resistance to ALS-associated degeneration. Cell Stem Cell 25:193-209.

Turer EE, Tavares RM, Mortier E, Hitotsumatsu O, Advincula R, Lee B, Shifrin N, Malynn BA, Ma A (2008) Homeostatic MyD88-dependent signals cause lethal inflammation in the absence of A20. J Exp Med 205:451-464.

Van Kampen JM, Baranowski DC, Robertson HA, Shaw CA, Kay DG (2015) The progressive BSSG rat model of Parkinson's: recapitulating multiple key features of the human disease. PLoS One 10:e0139694.

Vance C, Rogelj B, Hortobágyi T, De Vos KJ, Nishimura AL, Sreedharan J, Hu X, Smith B, Ruddy D, Wright P, Ganesalingam J, Williams KL, Tripathi V, Al-Saraj S, Al-Chalabi A, Leigh PN, Blair IP, Nicholson G, de Belleroche J, Gallo JM, et al. (2009) Mutations in FUS, an RNA processing protein, cause familial amyotrophic lateral sclerosis type 6. Science 323:1208-1211.

Volonte C, Apolloni S, Parisi C (2015) MicroRNAs: newcomers into the ALS picture. CNS Neurol Disord Drug Targets 14:194-207.

Wakabayashi K, Mori F, Kakita A, Takahashi H, Utsumi J, Sasaki H (2014) Analysis of microRNA from archived formalin-fixed paraffin-embedded specimens of amyotrophic lateral sclerosis. Acta Neuropathol Commun 2:173.

Wang Q, Johnson JL, Agar NY, Agar JN (2008) Protein aggregation and protein instability govern familial familial amyotrophic lateral sclerosis patient survival. PLoS Biol 6:e170.

Williams AH, Valdez G, Moresi V, Qi X, McAnally J, Elliott JL, Bassel-Duby R, Sanes JR, Olson EN (2009) MicroRNA-206 delays ALS progression and promotes regeneration of neuromuscular synapses in mice. Science 326:1549-1554.

Wilson JM, Khabazian I, Wong MC, Seyedalikhani A, Bains JS, Pasqualotto BA, Williams DE, Andersen RJ, Simpson RJ, Smith R, Craig UK, Kurland LT, Shaw CA (2002) Behavioral and neurological correlates of ALS-parkinsonism dementia complex in adult mice fed washed cycad flour. Neuromolecular Med 1:207-221.

Xu YF, Gendron TF, Zhang YJ, Lin WL, D'Alton S, Sheng H, Casey MC, Tong J, Knight J, Yu X, Rademakers R, Boylan K, Hutton M, McGowan E, Dickson DW, Lewis J, Petrucelli L (2010) Wild-type human TDP-43 expression causes TDP-43 phosphorylation, mitochondrial aggregation, motor deficits, and early mortality in transgenic mice. J Neurosci 30:10851-10859.

Yamanaka K, Chun SJ, Boillee S, Fujimori-Tonou N, Yamashita H, Gutmann DH, Takahashi R, Misawa H, Cleveland DW (2008) Astrocytes as determinants of disease progression in inherited amyotrophic lateral sclerosis. Nat Neurosci 11:251-253.

Yokoseki A, Shiga A, Tan CF, Tagawa A, Kaneko H, Koyama A, Eguchi H, Tsujino A, Ikeuchi T, Kakita A, Okamoto K, Nishizawa M, Takahashi H, Onodera O (2008) TDP-43 mutation in familial amyotrophic lateral sclerosis. Ann Neurol 63:538-542.

Zhou F, Guan Y, Chen Y, Zhang C, Yu L, Gao H, Du H, Liu B, Wang X (2013) miRNA-9 expression is upregulated in the spinal cord of G93A-SOD1 transgenic mice. Int J Clin Exp Pathol 6:1826-1838.

Zhou F, Zhang C, Guan Y, Chen Y, Lu Q, Jie L, Gao H, Du H, Zhang H, Liu Y, Wang X (2018) Screening the expression characteristics of several miRNAs in G93A-SOD1 transgenic mouse: altered expression of miR-124 is associated with astrocyte differentiation by targeting Sox2 and Sox9. J Neurochem 145:51-67.